Title
Quantitative analysis of the diffusion of hydrogen peroxide through teeth

Author
Petersen, Brenden Kyle

Publication Date
2012

Peer reviewed|Thesis/dissertation

UNIVERSITY OF CALIFORNIA

Los Angeles

Quantitative analysis of the diffusion of hydrogen peroxide through teeth

A thesis submitted in partial satisfaction

of the degree requirements for the degree Master of Science

in Biomedical Engineering

by

Brenden Kyle Petersen

2012

ABSTRACT OF THE THESIS

Quantitative analysis of the diffusion of hydrogen peroxide through teeth

by

Brenden Kyle Petersen

Master of Science in Biomedical Engineering

University of California, Los Angeles, 2012

Professor Benjamin M. Wu, Chair

Dental whitening is a rapidly expanding cosmetic industry. However, due to lack of quantitative analysis regarding the mass transport of hydrogen peroxide through teeth, clinical parameters like application time remain largely empirical, and little is known regarding the extent to which whitening should be supplemented with heat, light, or other activators. This study presents an experimental method fit to a mathematical model that can be used to determine the physical parameters of peroxide transport in teeth for various external conditions, sufficiently general to extend to platforms other than dental whitening. Using these methods, the diffusivity of hydrogen peroxide through bovine enamel at room temperature was determined to be $5.83\times10^{-8} \pm 0.50\times10^{-8}$ cm^2/s, with thermal activation energy of 48.30 ± 1.34 kJ/mol. These results, in combination with clinical studies, can be used to optimize clinical whitening parameters and serve as a basis for additional studies aimed at controlling peroxide diffusion, ultimately minimizing harmful side-effects while maintaining whitening efficacy.

The thesis of Brenden Kyle Petersen is approved.

Daniel T. Kamei

Gerard C. L. Wong

Benjamin M. Wu, Committee Chair

University of California, Los Angeles

2012

Table of Contents

Part 1 – Background and motivation

1.1 – Diffusion of small molecules in liquid-saturated porous media

Small molecules readily diffuse through porous media. Compared to bulk diffusion, diffusion in porous media is limited to the space within the pores. Furthermore, the medium's porosity, tortuosity, and constrictivity may restrict the paths available for diffusion, which affects mass transport. When the porous medium is saturated with liquid, the mean free path of solutes is relatively small compared to the pore size. There are few collisions with pore walls, thus transport follows Fick's laws of diffusion. Here, unless otherwise specified, all diffusion processes refer specifically to diffusion in liquid-saturated porous media.

1.1.1 – Fick's first law of diffusion

Fick's laws of diffusion describe the diffusion process mathematically. According to Fick's first law, at steady-state:

$J = -D\nabla c$,

where J is the diffusive flux, D is the substance's diffusivity, c is the concentration. The equation assumes a constant density solution and a dilute solution (in which solutes do not strongly interact). According to the equation, a substance diffuses from regions of high concentration to regions of low concentration, with magnitude proportional to the concentration gradient.

1.1.2 – Fick's second law of diffusion and the conservation of species equation

Fick's second law describes concentration changes over time:

$$\frac{\partial c}{\partial t} = \nabla \cdot (D \nabla c),$$

where t is time. This equation is appropriate in the absence of convection and chemical reactions. Like Fick's first law, this equation also assumes a constant density solution and a dilute solution.

Generalizing Fick's second law, including both convection and chemical reactions, the conservation of species equation is:

$$\frac{\partial c}{\partial t} + \nabla \cdot \vec{v} = \nabla \cdot (D \nabla c) + R_V,$$

where $\vec{v}$ is the convection velocity and R_V is the net rate of formation of a species per unit volume. The equation inherits the same assumptions as Fick's second law: a constant density solution and a dilute solution. In this form of the equation, diffusivity need not be spatially constant; however, this is a common simplification to the equation (see section 2.2.1).

1.2 – Diffusivity

Diffusivity (specifically mass diffusivity, also called diffusion coefficient) is a measure of the tendency for one species to diffuse into another. From Fick's first law, it is also the proportionality constant between mass flux and concentration gradient. Bulk diffusivity is a property of two species: the diffusate (molecule diffusing) and the

surrounding solvent. However, in porous media, the membrane environment through which the diffusate diffuses also affects transport, and thus the observed diffusivity differs from the bulk diffusivity. The SI units for diffusivity are m^2/s, but most studies report values in cm^2/s.

Diffusivity is often empirically determined to follow a temperature dependence given by the Arrhenius equation:

$$D = D_0 \exp\left(\frac{-E_A}{RT}\right),$$

where D is diffusivity, D_0 is the pre-exponential factor (in the same units as diffusivity), E_A is the activation energy (in kJ/mol) for diffusion, and R is the ideal gas constant (equal to 8.314 J/mol-K), and T is the absolute temperature (in K). Traditionally used to describe the temperature dependence of reaction rate constants (*1*), the Arrhenius equation has also been empirically determined to hold for the diffusivity of aqueous diffusates under a variety of experimental conditions (*2-5*). The activation energy represents a thermodynamic energy barrier to diffusion. Physically, this represents the energy sufficient to overcome attractive forces between the diffusate and the solvent or porous media (*6*). Thus, a process found to follow the form of the Arrhenius equation is known as a thermally activated process.

1.2.1 – Apparent and effective diffusivity

Diffusivity in porous media is affected by many factors of the membrane. Diffusion occurs through the pore spaces, thus porosity available for transport affects diffusivity. The distinction “available for transport” is necessary because some pores many not penetrate

completely from one end of the membrane to the other; thus, some pores are "dead ends" through which diffusion cannot occur. Porosity available for transport accounts for this difference. The diffusion path may not occur directly from one side of the membrane to the other, thus the tortuosity of the pores also affects diffusivity. Finally, the resistance to transport increases when the diameter along a pore varies, thus the constrictivity of the pores also affects diffusivity (*7*). Porosity available for transport, tortuosity, and constrictivity are all dimensionless factors between zero and unity.

Depending on the experimental setup used to determine diffusivity in porous media, there are various types of diffusivity. The apparent diffusivity D_a is obtained from exposing a membrane to a known concentration gradient (*8*). "Apparent" indicates that the diffusate concentrations are assumed to be equal to those just outside the membrane, while the true concentration just inside the membrane is decreased due to excluded volume between pores. Thus, D_a is decreased by a factor of the membrane's porosity available for transport. D_a also is affected by the tortuosity of the pores, as it assumes a diffusion path directly from one side of the membrane to the other, although the true diffusion path may be longer.

The effective diffusivity D_e "is a measure of the rate at which a front of diffusate moves through the material and is measured by following penetration of diffusate into the material or by clearance from a sample pre-equilibrated with the diffusate" (*9*). "Effective" indicates that the tortuosity of the pores is not taken into account, and the true diffusion path may be longer. D_e is unaffected by the membrane's porosity; however, it is affected by any reversible binding with pore surfaces. De can also be obtained by multiplying D_a by a partition coefficient that takes into account the porosity available for transport (*8*).

Here, based on the experimental setup (see section 3.3), *D* will always refer to the apparent diffusivity of aqueous hydrogen peroxide through enamel (or dentin, when specified).

1.2.2 – Applications of diffusivity for various platforms

Determining the value of diffusivity has important applications for various platforms. For example, diffusivity may be a key parameter in bone fracture or osteoporosis that can be useful in early diagnosis. In this case, diffusion-weighted magnetic resonance imaging can also be used to quantify diffusion (*10*). For civil engineering applications, the diffusivity of concrete is an indicator of the service life-time of concrete structures (*11*). In the food industry, the diffusivity of polymer/clay nanocomposites used for food packaging may help predict its barrier properties (*12*).

Diffusivity has various applications for tooth whitening. Currently, whitening parameters like application time and renewal time remain empirical (*13*). The diffusivity of bleaching molecules through teeth could be used to determine the maximum safe application time before risk of tooth sensitivity or irreversible damage, or the optimal renewal time between applications, as these both currently remain empirical.

1.3 – Tooth whitening

1.3.1 – Overview

Tooth whitening—also called dental bleaching—is a common dental cosmetic procedure. For most tooth whitening procedures, a bleaching agent—traditionally hydrogen peroxide (H_2O_2) or carbamide peroxide—is externally applied to the tooth surface. The bleaching agent diffuses into the tooth, reacting along the way with exogenous stain molecules present within enamel and dentin. Since enamel is thinner and more translucent than dentin, the overall color of the tooth is largely determined by the color of dentin (*14*). Thus, dentin is the primary target for bleaching.

1.3.2 – Bleaching mechanism

While the exact reaction mechanisms are unknown, the bleaching mechanism involves oxidation of exogenous stain molecules by dissociation products of hydrogen peroxide (*15, 16*). Exogenous stain molecules are organic compounds with conjugated chains of alternating single or double bonds (*16*). The portion of the stain molecule responsible for the stain's color is called a chromophore. Decolorizing of a chromophore occurs by destroying one or more double bonds or otherwise interrupting its conjugated chain (*16*). The reaction is thought to occur via hydroxyl radicals (·OH), perhydroxyl radicals ($HO_2\cdot$), and/or perhydroxyl anions (HO_2^-) (*15, 16*).

1.3.3 – Tooth whitening methods

There three major types of peroxide-based tooth whitening methods: in-office, at-home, and over-the-counter (OTC). In-office bleaching typically involves a hydrogen peroxide-based gel formulation applied by a dental professional for 30 – 60 minutes. In-office techniques use concentrations of up to 25 – 35% hydrogen peroxide (*16*). In-office bleaching may be accelerated using heat or light activation. At-home bleaching (also called nightguard vital bleaching) techniques typically use less concentrated gel formulations of either hydrogen peroxide (around 3.5 – 7.5%) or carbamide peroxide (around 10 – 20%). Under the supervision of a dental professional, at-home bleaching involves applying peroxide gel into a custom tray, or impression of the patient's teeth from around 1 – 2 hours (daytime whiteners) or overnight (nighttime whiteners) for a period of around 1 – 2 weeks. Finally, OTC whiteners use even smaller hydrogen peroxide or carbamide peroxide concentrations in a thin strip or wrap that is fitted to the surface of the teeth. These are typically applied for around 30 minutes each for around 1 – 2 weeks.

The efficacy of these gel-based methods is summarized in Figure 1 (*17*). The dependent axis represents change using Trubyte Bioform Shade guide, a common clinical measure of whitening efficacy. Clearly, under the conditions used in these experiments, at-home techniques have the highest whitening efficacy. Another study found that, to achieve a given whitening efficacy, in-office treatment requires 3.15 cycles of treatment, at-home techniques require 7.15 cycles, and OTC methods require 31.85 cycles (*18*).

For many gel-based methods, carbamide peroxide is used instead of hydrogen peroxide. Carbamide peroxide is an adduct of urea and hydrogen peroxide; in water it

releases free hydrogen peroxide. Based on molecular weights, a carbamide peroxide formulation is approximately 36% hydrogen peroxide. Thus, a 10% carbamide peroxide formulation is approximately equal to a 3.6% hydrogen peroxide formulation.

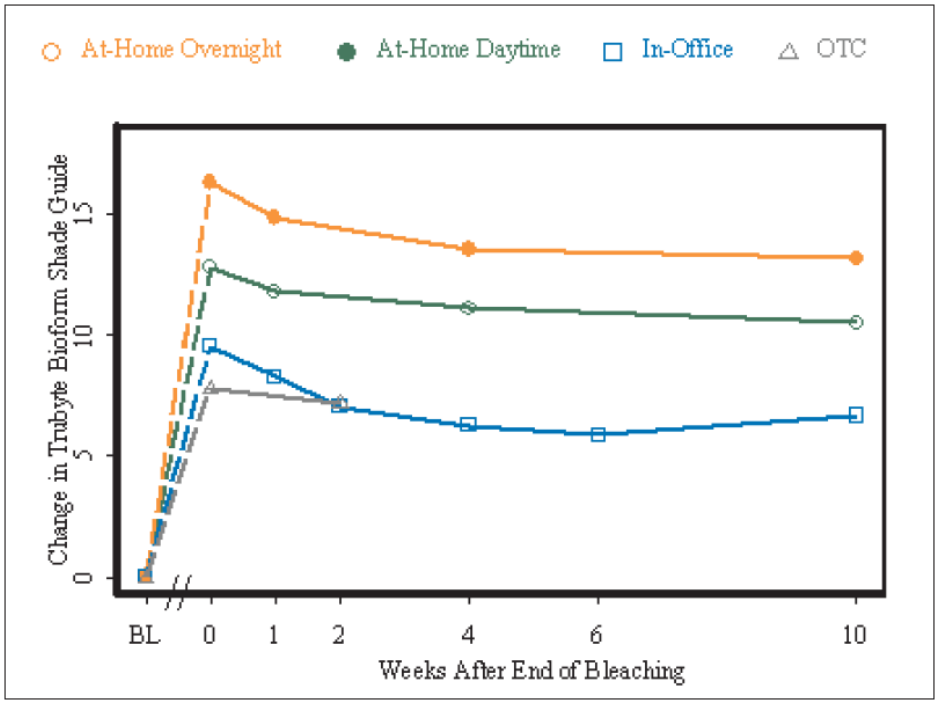

Figure 1. Whitening efficacy of various gel-based tooth whitening methods (*17*).

Other non-peroxide-based tooth whitening methods can include extrinsic stains on the surface of the tooth. Whitening toothpastes contain chemicals like sodium citrate that may white teeth (*19*). One whitening toothpaste containing silica shifts the tooth from a yellow to blue color, contributing to the self-perception of tooth whiteness (*20*). Microabrasion techniques utilizing silicon carbide and hydrochloric acid can remove surface discolorations (*21*). Here, tooth whitening will refer specifically to peroxide-based whitening methods.

1.3.4 – Clinical significance

Tooth whitening, including both at-home and in-office applications, is becoming increasingly prevalent. One survey demonstrated that 32% of the population is dissatisfied with their teeth color, and 27% believes that cosmetic dentistry can improve their quality of life (*22*). The market for United States dental hygiene and oral care exceeded $1.6 billion in 2010 and is projected to reach $2 billion by 2017, and tooth whitening applications largely fuel this growth (*23*).

1.3.5 – Risks of tooth whitening

Tooth sensitivity is a common limitation of dental whitening that leads to patient discomfort and possible early termination of treatment (*24-28*). A comparative study of three brands of 10% carbamide peroxide at-home techniques reported hypersensitivity occurring in 38-78% of patients (*24*). For in-office techniques using 30% hydrogen peroxide accompanied with heat, hypersensitivity increased to 67-78% (*25, 26*). In one study, 20% of those who experienced hypersensitivity terminated treatment early due to discomfort (*24*). Sensitivity usually persists for up to four days after treatment (*25, 27*); however, some studies report sensitivity persisting as late as 39 days after treatment (*24, 28*).

Tooth sensitivity is caused by pulpal damage, which can be reversible or irreversible. While most proper tooth whitening applications do not result in irreversible pulpal damage, clinical causes of irreversible damage have been reported (*29*). One such case reported pulpal necrosis and periradicular periodontitis, resulting in root canal

therapy (*30*). Risk of irreversible pulpal damage increases dramatically when whitening therapy is supplemented with heat (*31*). Intracoronal bleaching has also been found to lead to inflammatory-mediated external root resorption (*32*).

1.4 – Tooth morphology

1.4.1 – Enamel

Human teeth have two main layers: enamel and dentin. Comprising the out layer of the tooth, human enamel is primarily composed of hydroxyapatite. The basic unit of enamel is the enamel rod, consisting of tightly packed, organized hydroxyapatite crystals. Enamel rods, averaging 5 μm in diameter and up to 3 mm in length, are oriented perpendicular to the underlying dentin (*33*). Moderate anisotropy of the enamel rod organization has been found, which increases crack resistance both along and across the dominant rod direction (*34*). While the enamel layer is acellular, it contains various proteins. Amelogenin is the principal protein found in developing enamel, and is thought to regulate the growth and organization of hydroxyapatite crystals (*35*). Once mineralization of enamel is complete in the developing tooth, the enamel layer is up to 2.5 mm thick, thickest at the cusp of the tooth and thinnest at the cementoenamel junction (*36*). It typically ranks 5 on Mohs hardness scale and has a Young's modulus of around 83 GPa, although these values depend on factors such as gender and age of tooth (*37*).

The enamel layer is semitranslucent, with color varying from light yellow to grayish white. Enamel contains pores on the order of 2 nm in radius, and the water content of enamel is approximately 1% w/w (or 3% v/v) (*38*). These nanopores contribute to the

transport properties of enamel. Diffusivity of fluoride in the enamel pores has been found to be 1.0 x 10^{-5} cm^2/sec (*39*). Diffusion of hydrogen peroxide through the enamel layer of intact teeth is known to occur within 15 minutes of exposure, but its exact diffusivity has not yet been quantified.

1.4.2 – Dentin

Underlying the enamel layer, dentin is composed of 70% hydroxyapatite by weight, 20% organic material, and 10% water (*33*). Around 5 mm thick in humans, the dentin layer is yellow in color, and its semi-translucency contributes to the overall color of the tooth. Compared to enamel, dentin is much less mineralized and contains a larger proportion of organic material.

Dentin contains microscopic channels called dentinal tubules that extend radially outward from the pulpal side of the dentin to the dentin-enamel interface. The diameter of the tubules ranges from 1 – 3 μm, decreasing as the tubule radiates from the pulpal side to the enamel side; similarly, the number density of tubules decreases from over 45,000/mm^2 at the pulpal side to less than 20,000/mm^2 at the dentin-enamel interface (*40*). The tubules contain cells called odontoblasts that secrete dentin. As a result of the fluid-filled dentinal tubules, dentin has a much smaller Young's modulus than enamel. The Young's modulus for intertubular dentin (between dentinal tubules) ranges from 17 – 22 GPa, increasing with distance away from the pulp, and the Young's modulus for peritubular dentin (surrounding dentinal tubules) is approximately 30 GPa (*41*). Dentin contains pores on the order of 1 μm in diameter, and the water content of dentin is approximately 10% w/w (or 21% v/v) (*38,*

42). These micropores, as well as the dentinal tubules, contribute to the transport properties of dentin. In one study, the permeability of dentin ranged from 2.8 x 10^{-6} cm^2/min for ^{131}I-albumin to 2.7 x 10^{-4} cm^2/min for ^3H_2O (*43*). While diffusion of hydrogen peroxide through dentin has been shown to occur faster than enamel, its exact diffusivity has not yet been quantified.

1.4.3 – Pulp

Underlying both enamel and dentin and comprising the center of the tooth is the pulp. The cavity of the tooth filled with pulp is called the pulp chamber. The pulp is composed of connective tissue and cells called odontoblasts that create new dentin. It contains both nerves and blood vessels. Tooth sensitivity largely results from interaction between hydrogen peroxide and the pulp tissue.

1.5 – Diffusion of hydrogen peroxide in teeth

1.5.1 – Factors affecting peroxide diffusion

Hydrogen peroxide has been shown to readily diffuse through both enamel and dentin, with transport properties depending on many external conditions (*44, 45*). Even concentrations as low as 5% (w/v) hydrogen peroxide diffuse through both and enamel and dentin and into the pulp chamber within 15 – 30 minutes (*44, 46*). Multiple studies indicated that increasing peroxide concentration from 10% to 35% results in approximately doubling the amount of peroxide penetrating into the pulp chamber (*47-49*).

Increasing the temperature within the range of 24 °C to 47 °C also increased peroxide diffusion (*50*). The duration of hydrogen peroxide exposure to teeth also affects diffusion. Studies demonstrate significant increases in diffusion with increased exposure time for both small scale (minutes to hours) and large scale (hours to days) (*50, 51*). Light activation using LED and halogen lamps can also increase peroxide diffusion. One study found that LED and halogen activation produced similar levels of peroxide penetration (*52*). Chemical activators can decrease peroxide penetration while maintaining the same bleaching efficacy. One study found that manganese gluconate (0.01 g, or 0.025% inside the peroxide gel) and ferrous sulphate (0.0016 g, or 0.004% inside the gel) significantly decreased peroxide penetration (*53*). Due to the radial dependence of dentinal tubule diameter, diffusion in dentin is found to occur faster near the pulp chamber and slower near the enamel, although this has not yet been validated with hydrogen peroxide (*54*). Another study determined that peroxide diffusion was faster in human teeth than bovine teeth, attributing the results to smaller dentinal tubule diameter and larger dentin area between tubules (*55*). Finally, younger teeth yield higher levels of peroxide penetration than older teeth due to older teeth's reduced dentinal tubule diameter (*51*).

1.5.2 – Pulp chamber penetration studies

Experiments involving the diffusion of hydrogen peroxide in teeth can be separated into two categories: pulp chamber penetration studies and cylindrical disc diffusion studies. Pulp chamber penetration studies generally expose hydrogen peroxide to the enamel of extracted teeth with the pulp removed (*44, 46-50, 52, 55, 56*). This method

introduces many experimental variables like minimum tooth thickness, surface area exposed to peroxide, and volume of pulp chamber. On the other hand, this method accurately reflects the clinical tooth whitening procedure. Therefore, this method is preferable for determining clinical results (like mass of peroxide penetrating the pulp chamber within 30 minutes), but is not useful for determining physical parameters of peroxide transport (like diffusivity).

1.5.3 – Cylindrical disc diffusion studies

Cylindrical disc diffusion studies prepare cylindrical discs of enamel and/or dentin, expose one side of the disc to hydrogen peroxide, and expose the other side of the disc to a water reservoir (*51, 53, 57, 58*). This method tends to control experimental variables well, although it does not accurately reflect the clinical tooth whitening procedure. Therefore, this method is preferable for determining physical parameters of peroxide transport, but is not useful for determining clinical results.

1.6 – Limitations of existing literature

1.6.1 – Inability for cross-experiment comparisons

Many existing studies lack appropriate controls or adequate standards, making it difficult to interpret results across experimental methods. This is especially true for pulp chamber penetration studies. For example, many studies did not specify membrane

thickness or surface area exposed to hydrogen peroxide (*44, 46-50, 52, 56*). Thus, results like "mass of peroxide penetrating the pulp chamber within 30 minutes" cannot be appropriately compared across multiple experiments.

While most cylindrical disc diffusion studies specify the experimental parameters, cross-experiment comparisons are still generally not appropriate because there are no standards for experimental parameters. For example, diffusion of 30% peroxide through a 1.0 mm-thick disc cannot be easily compared to diffusion of 10% peroxide through a 2.0 mm-thick disc. In order for such results to be comparable, physical parameters of peroxide transport must be determined, as well as their dependence on experimental parameters. This requires a mathematical model to back out physical parameters; however, existing cylindrical disc diffusion studies are not appropriately designed for backing out physical parameters (see section 3.1.1).

1.6.2 – Lack of quantitative analysis

Currently, no studies provide an experimentally derived diffusivity of hydrogen peroxide through enamel or dentin. In fact, the majority of studies simply measure the amount of peroxide that penetrates a sample at one or more specified time points (*44-50, 52, 53, 55*). While statistically significant differences are often found between experimental groups (e.g. 10% hydrogen peroxide versus 30% hydrogen peroxide), few attempts are made to further quantify diffusion or compare experimental results with mass transport theory.

Some mass transport texts provide values for peroxide diffusivity; however, upon further investigation, all such texts make certain assumptions that invalidate the accuracy of the value. For example, one text assumes that the diffusivity of hydrogen peroxide in teeth is equal to that of water in bone (*59*). It also assumes that diffusivity of hydrogen peroxide is equal in enamel and dentin, which is experimentally known to be false.

A recent study claims to obtain the transport coefficient (i.e. diffusivity) of peroxide in teeth from existing literature; however, the value is not stated, and specific references are not provided (*60*). Therefore, it is possible that this study used an inappropriate diffusivity value pulled from a text. Alternatively, the study could have backed out the value of diffusivity from existing experimental data; however, this is unlikely because most diffusion studies do not have experimental designs appropriate for backing out physical parameters.

Other unknowns of peroxide transport include the threshold level of pulp chamber penetration that is acceptable before excessive tooth sensitivity or irreversible pulpal damage occurs. Further insight is also needed concerning the connection between diffusion and reaction of peroxide in teeth.

1.7 – Need for quantitative analysis

Improved quantitative analysis of peroxide diffusion and reaction in teeth will greatly aid the clinical setting by providing a scientific basis for choosing whitening parameters. Currently, parameters like application time and optimal renewal time remain empirical, but this can be overcome with quantitative studies involving multiple time

points (*51*). Quantitative analysis, coupled with results from clinical studies, will facilitate optimizing the inherent balance between tooth sensitivity and whitening efficacy. For example, if a clinical study determines the threshold level of peroxide (if any) to penetrate the pulp chamber before causing risk of damage or sensitivity, quantitative transport studies can determine the maximum peroxide concentration and application time below this threshold, thereby maximizing whitening while maintaining patient safety.

Quantitative characterization of peroxide transport in teeth will also facilitate controlling the transport. Simple questions like, "Should diffusion and/or reaction be sped up?" currently remain unanswered. Determining whether diffusion, reaction, or neither is rate-limiting in the whitening process will motivate which steps to take in controlling peroxide transport. For example, if diffusion is rate-limiting (i.e. relatively slow compared to reaction), the reaction is fast and thus diffusion should be controlled to limit pulp chamber penetration. On the other hand, if neither is rate-limiting (i.e. diffusion and reaction rate are comparable), then perhaps a compromise between tooth sensitivity and whitening efficacy must be adopted. Finally, once both diffusion and reaction can be quantitatively characterized, researchers can develop methods to decrease tooth sensitivity without compromising whitening efficacy and/or increase whitening efficacy without exacerbating tooth sensitivity (see section 6.3).

Part 2 – Mathematical model

The goal is to develop a mathematical model that 1) can be used to back out physical parameters (i.e. diffusivity, rate constant) and 2) can be emulated in the laboratory. The first goal is necessary so that meaningful information about hydrogen peroxide diffusion through enamel can be gained from the model. The second goal is necessary so that the model can appropriately be fitted to actual experimental results. For example, diffusion of hydrogen peroxide into a cylindrical shell of enamel would allow for simple determination of physical constants, but is not feasible in the laboratory due to enamel's size and shape limitations.

2.1 – Schematic representation

The schematic of the diffusion-reaction of hydrogen peroxide in a semi-permeable membrane (enamel or dentin) is shown in Figure 2. The membrane has known area A and known thickness L. It is oriented such that diffusion occurs in the $+x$ direction. One end of the membrane (at $x = 0$) is exposed to hydrogen peroxide gel of known concentration c_0. The other end of the membrane (at $x = L$) is exposed to pure water.

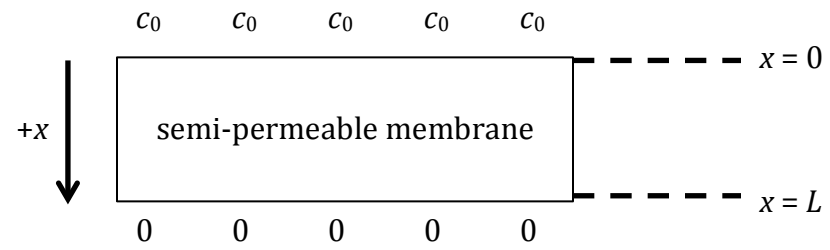

Figure 2. Schematic of diffusion-reaction of hydrogen peroxide in a semi-permeable membrane.

2.2 – Setting up the conservation of species equation

The diffusion-reaction of hydrogen peroxide through a semi-permeable membrane (enamel or dentin) can be modeled using the conservation of species equation in Cartesian coordinates:

$$\frac{\partial c}{\partial t} + \nabla \cdot \vec{v} = \nabla \cdot (D \nabla c) + R_V$$

In this equation, c represents the concentration of the diffusate (hydrogen peroxide), t represents time, $\vec{v}$ represents the convection velocity, D represents the diffusivity of the diffusate in the membrane, and R_V represents the rate of homogenous reaction (positive for production and negative for consumption).

2.2.1 – Simplifications to the equation

The following simplifications can be made to the conservation of species equation:

- One-dimensional diffusion
- No convection
- Constant diffusivity

- Pseudo-first order, homogeneous consumption reaction

One-dimensional diffusion:

Based on the geometry of the problem, there are no concentration gradients in the y or z direction. Thus, diffusion only occurs one-dimensionally, in the x direction. As a result, concentration is only a function of t and x, not t and all three spatial dimensions. Also, thee gradient operators can be simplified to partial derivatives in the x direction.

No convection:

Since the experimental process takes place in stagnant water, convection does not contribute to hydrogen peroxide transport. Thus, $\vec{v} = 0$.

Constant diffusivity:

Enamel is known to be relatively homogeneous, so its diffusivity can be treated as constant. Thus, D can be pulled out of the gradient operator. Note that this is not the case for dentin, which contains dentinal tubules that decrease in diameter from the pulp to buccal side of the tooth. However, for thin slabs of dentin all taken from the same end of the tooth (pulpal or buccal), diffusivity will be approximated as constant.

Pseudo-first order, homogeneous consumption reaction:

Hydrogen peroxide irreversible reacts with stain molecules in both enamel and dentin. The rate of consumption is proportional to the concentration of hydrogen peroxide. The proportionality constant is k, the reaction rate constant. Thus, the R_V term becomes $-kc$.

The resulting, simplified conservation of species equation is:

$$\frac{\partial c}{\partial t} = D\frac{\partial^2 c}{\partial x^2} - kc$$

2.2.2 – Boundary and initial conditions

The simplified equation is second order in space and first order in time, requiring two boundary conditions and one initial condition.

The boundary conditions are of the Dirichlet type, representing an infinite source and infinite sink. One side of the membrane (at $x = 0$) is exposed to hydrogen peroxide gel of known concentration c_0. The other side of the membrane (at $x = L$) is exposed to pure water. Strictly speaking, the source and sink are not infinite. That is, there is a decreasing amount of peroxide in the gel as it diffuses through the membrane, and there is a nonzero amount of peroxide on the opposite side of the membrane once peroxide diffuses through. However, the ratio of peroxide concentration from the source to sink side is very large (four orders of magnitude), so the boundary concentrations can be treated as constants. The validity of these boundary conditions is examined in greater detail in section 5.1.

In equation form, the boundary conditions are:

1. Infinite source: $c(x = 0, t) = c_0$
2. Infinite sink: $c(x = L, t) = 0$

The initial condition is: $c(x, t = 0) = 0$. That is, at the beginning of the experiment ($t = 0$), the membrane is saturated with water and has not been exposed to hydrogen peroxide.

The following set of conditions summarize the initial-boundary-value problem:

$$\begin{cases} \dfrac{\partial c}{\partial t} = D\dfrac{\partial^2 c}{\partial x^2} - kc \\ c(x = 0, t) = c_0 \\ c(x = L, t) = 0 \\ c(x, 0) = 0 \end{cases}$$

2.3 – Necessity of implementing Fick's first law

Solving the conservation of species equation yields the concentration profile of the diffusate within the membrane. This is useful when the concentrations of diffusate within the membrane thickness can be directly measured. However, it is not experimentally feasible to measure the hydrogen peroxide concentration at any point within the membrane. Even the surface concentration at the membrane-water interface is difficult to measure. Only the concentration inside the sink (water reservoir) can be measured directly.

To overcome this experimental limitation, Fick's first law can be used to calculate the theoretical mass flux (J) through the membrane, which is directly related to the concentration inside the sink (if the water reservoir is well-mixed). According to Fick's first law in one dimension,

$$J = -D\frac{\partial c}{\partial x}$$

Thus, at the membrane-water interface,

$$J(L,t) = -D\left.\frac{\partial c}{\partial x}\right|_{x=L}$$

In this expression, $J(L,t)$ represents the mass flux at the membrane-water interface at a given time. Note that it is only a function of time. The cumulative mass diffused through the membrane can be obtained by integrating the mass flux over time, and multiplying by the area of the membrane (A):

$$m(t) = \int_0^t J(L,t')\,dt' = -D\int_0^t \left.\frac{\partial c}{\partial x}\right|_{x=L} dt$$

It is this value that can be directly measured in the experiment, so solutions of the initial-boundary value problem (concentration profiles) will implement Fick's first law to obtain an expression for cumulative mass diffused through the membrane as a function of time. Furthermore, this mass will be used to back out physical constants from the model.

Note that, when solving the initial-boundary-value problem, the sink concentration was held constant at zero. Strictly speaking, the experimental sink concentration is greater than zero once some amount of hydrogen peroxide diffuses through the membrane. However, this concentration is very small compared to the source concentration (by a factor of six orders of magnitude); thus, the infinite source, infinite sink boundary conditions remain good approximations. The validity of these boundary conditions is examined in greater detail in section 5.1.

2.4 – Solving the conservation of species equation

Before solving the full initial-boundary-value problem, several simpler problems will first be solved to give greater insight into the full solution.

2.4.1 – Steady-state model without reaction

First, consider the same experimental setup at steady-state, ignoring the reaction. The problem simplifies to:

$$\begin{cases} 0 = D\dfrac{d^2c}{dx^2} \\ c(0) = c_0 \\ c(L) = 0 \end{cases}$$

Note that concentration now becomes a function of just one variable. Thus, partial derivatives can be replaced with whole derivatives.

The differential equation is solved by integrating both sides of the equation twice. The concentration profile for this problem is:

$$c(x) = c_0\left(1 - \frac{x}{L}\right)$$

Implementing Fick's first law, the cumulative mass diffused through the membrane is:

$$m(t) = \frac{c_0 ADt}{L}$$

Note that the concentration drops linearly across the membrane, and the mass increases linearly with time.

Normalizing by area and time, the flux across the membrane is a constant:

$$J = \frac{c_0 D}{L}$$

2.4.2 – Steady-state model with reaction

Next, the reaction term will be added back into the previous problem. The problem becomes:

$$\begin{cases} 0 = D\dfrac{d^2c}{dx^2} - kc \\ c(0) = c_0 \\ c(L) = 0 \end{cases}$$

The differential equation is a second-order, linear, homogeneous ODE with constant coefficients, and can be solved by finding the roots of the characteristic equation. The general solution to this differential equation is:

$c(x) = A\cosh\left(\sqrt{\frac{k}{D}}x\right) + B\sinh\left(\sqrt{\frac{k}{D}}x\right)$, where A and B are arbitrary constants.

Applying the boundary conditions, the concentration profile for this problem is:

$$c(x) = c_0\cosh\left(\sqrt{\frac{k}{D}}x\right) - c_0\sinh\left(\sqrt{\frac{k}{D}}x\right)\coth\left(\sqrt{\frac{k}{D}}L\right)$$

Implementing Fick's first law, the cumulative mass diffused through the membrane is:

$$m(t) = c_0 At\sqrt{kD}\left[\cosh\left(\sqrt{\frac{k}{D}}L\right)\coth\left(\sqrt{\frac{k}{D}}L\right) - \sinh\left(\sqrt{\frac{k}{D}}L\right)\right]$$

Using the identity $\cosh^2 x - \sinh^2 x = 1$,

$$m(t) = c_0 At\sqrt{kD}\,\mathrm{csch}\left(\sqrt{\frac{k}{D}}L\right)$$

Normalizing by area and time, the flux across the membrane is a constant:

$$J = c_0\sqrt{kD}\,\mathrm{csch}\left(\sqrt{\frac{k}{D}}L\right)$$

To validate the previous case with no reaction,

$$\lim_{k\to 0} m(t) = \frac{c_0 ADt}{L}$$

Note that the concentration profile is no longer linear, but the cumulative mass diffused through the membrane still increases linearly with time.

2.4.3 – Time-dependent model without reaction

Next, the time dependence will be reinstated, ignoring reaction. The problem becomes:

$$\begin{cases} \dfrac{\partial c}{\partial t} = D\dfrac{\partial^2 c}{\partial x^2} \\ c(x=0,t) = c_0 \\ c(x=L,t) = 0 \\ c(x,0) = 0 \end{cases}$$

The partial differential equation is solved by separation of variables (details provided in Appendix I). After implementing the initial and boundary conditions, the concentration profile is:

$$c(x,t) = c_0\left(1-\frac{x}{L}\right) - c_0\sum_{n=1}^{\infty}\frac{2}{n\pi}\sin\left(\frac{n\pi x}{L}\right)\exp\left[-D\left(\frac{n\pi}{L}\right)^2 t\right]$$

Implementing Fick's first law, the cumulative mass diffused through the membrane is:

$$m(t) = \frac{c_0 ADt}{L} + 2c_0 AL \sum_{n=1}^{\infty} \frac{(-1)^n}{(n\pi)^2} \left[1 - \exp\left[-D\left(\frac{n\pi}{L}\right)^2 t\right]\right]$$

Note that the concentration profile and mass are non-linear; however, in both cases the first term is equivalent to the solution of the analogous steady-state problem. Thus, the concentration profile and mass are decreased by some time-dependent amount. As $t \to \infty$, the concentration profile approaches that of the analogous steady-state problem, and the slope of the mass approaches that of the analogous steady-state problem.

2.4.4 – Time-dependent model with reaction

Finally, the full solution will be determined. Again, the problem is:

$$\begin{cases} \dfrac{\partial c}{\partial t} = D\dfrac{\partial^2 c}{\partial x^2} - kc \\ c(x=0,t) = c_0 \\ c(x=L,t) = 0 \\ c(x,0) = 0 \end{cases}$$

The solution to this problem can be found in terms of the case in which there is no reaction (Crank, 1975). In particular,

$$c(x,t) = \int_0^t kc^*(x,t')e^{-kt}dt' + c^*(x,t)e^{-kt},$$

where $c^*(x,t)$ solves the case for $k = 0$.

Using this formula and the solution from the previous problem, the concentration profile for this problem is:

$$c(x,t) = c_0\left(1 - \frac{x}{L}\right) - c_0 \sum_{n=1}^{\infty} \frac{2}{n\pi} \sin\left(\frac{n\pi x}{L}\right) \frac{D\left(\frac{n\pi}{L}\right)^2 \exp\left[-D\left(\frac{n\pi}{L}\right)^2 t - kt\right] + k}{D\left(\frac{n\pi}{L}\right)^2 + k}$$

Implementing Fick's first law, the cumulative mass diffused through the membrane is:

$$m(t) = \frac{c_0 ADt}{L} + \frac{2c_0 AD}{L} \sum_{n=1}^{\infty} (-1)^n \frac{D\left(\frac{n\pi}{L}\right)^2 \left\{1 + kt - \exp\left[-D\left(\frac{n\pi}{L}\right)^2 t - kt\right]\right\} + k^2 t}{\left[D\left(\frac{n\pi}{L}\right)^2 + k\right]^2}$$

The following table summarizes the solutions to the various cases:

Table 1. Summary of solutions to cases of the initial-boundary-value problem.

Time dependent?	With reaction?	Solution (cumulative mass diffused through membrane)
No	No	$m(t) = \frac{c_0 A D}{L} t$
No	Yes	$m(t) = c_0 A t \sqrt{kD}\ \operatorname{csch}\left(\sqrt{\frac{k}{D}} L\right)$
Yes	No	$m(t) = \frac{c_0 A D t}{L} + 2 c_0 A L \sum_{n=1}^{\infty} \frac{(-1)^n}{(n\pi)^2} \left[1 - \exp\left[-D \left(\frac{n\pi}{L}\right)^2 t \right] \right]$
Yes	Yes	$m(t) = \frac{c_0 A D t}{L} + \frac{2 c_0 A D}{L} \sum_{n=1}^{\infty} (-1)^n \frac{D \left(\frac{n\pi}{L}\right)^2 \left\{ 1 + kt - \exp\left[-D \left(\frac{n\pi}{L}\right)^2 t - kt \right] \right\} + k^2 t}{\left[D \left(\frac{n\pi}{L}\right)^2 + k \right]^2}$

Solutions summarized in Table 1 will be repeatedly referenced using two criteria: 1) time-dependent versus steady state and 2) with reaction or without reaction.

2.5 – Backing out physical parameters

Software programs were developed to back out the physical parameters from the models (i.e. diffusivity). For the steady-state model with reaction, diffusivity must be solved for numerically. To facilitate many calculations in parallel, a C++ program was developed to numerically determine diffusivity values based on experimental results (see Appendix II.1 for annotated code).

For the time-dependent model with reaction, a non-linear least-squares regression was performed. In the absence of software the can handle both non-linear regression and summation notation, a C++ program was developed to computationally determine diffusivity and rate constant (see Appendix II.2 for annotated code). The user inputs known experimental parameters into the program, as well as measured values of cumulative mass diffused over time. Using the solution to the initial-boundary-value problem, the program determines the value of diffusivity corresponding to the largest calculated coefficient of determination (R^2).

Part 3 – Experimental methods

3.1 – Goals

There are three goals of the experimental setup.

3.1.1 – Goal 1: appropriate fit to mathematical model

Firstly, the experimental setup should appropriately fit the mathematical model so that physical parameters (like diffusivity) can be determined from experimental data. The physical constraints of the experimental setup must match the boundary conditions (infinite source and infinite sink) of the mathematical model. The experimental setup must also reflect the simplifications to and assumptions in the conservation of species equation. By creating such an experimental setup, parameters backed out of the mathematical model will reflect true, physical parameters.

While the experimental setup must match the mathematical model for physical parameters to be meaningful, note that certain experimental conditions need not match clinical—or even physiological—values to be physically meaningful. For example, the clinical time scale for tooth whitening application is about one hour, yet the diffusion experiment runs for over 24 hours. Despite this order of magnitude difference, the end goal is to determine the physical parameters of enamel. Such parameters are functions of the diffusate (hydrogen peroxide) and membrane (enamel or dentin)—not the time scale used. Thus, adhering to clinical time scales is not necessary. As another example, the temperature

range (used in the experimental setup to determine physical parameters like activation energy) need not fall within physiological ranges.

3.1.2 – Goal 2: cross-experiment reproducibility

Secondly, the experimental setup should be easily reproducible across experiments, such that the results do not depend on the parameters of the study. It should be easy to alter certain environmental conditions (e.g. temperature or concentration). It should also be easy for other researchers to reproduce the experiment. This facilitates meaningful cross-experiment comparisons of results. As one study points out, "Only comparisons among studies relying on *D* (diffusion coefficient) or *P* (permeability parameter) are valid because this calculation cancels out the parameters of the study such as remaining dentin thickness or initial concentration" (*51*).

3.1.3 – Goal 3: platform-independent generality

Thirdly, the experimental setup should be general enough to easily extend to other platforms. While this experiment only considers the diffusion of hydrogen peroxide in enamel or dentin, the experimental setup should be easily extended to the diffusion of other diffusates in other porous media.

3.2 – Sample preparation

Eighteen bovine central incisors without noticeable defects were obtained (Tri-State Beef CO, Cincinnati, OH). Teeth were individually cut into cylindrical discs with the following procedure:

Teeth were first sectioned using a separating disc and dental hand drill (NSK, Kanuma, Japan) and shaped into cylindrical discs using a diamond-coated burr and dental hand drill (Henry Schein, Melville, NY). Sections were taken parallel to the surface of the tooth. The resulting cylindrical discs were about 7 mm in diameter and a few millimeters in thickness. The cylindrical discs were then thinned to 1.2 mm using water-cooled abrasive grit (grit size 125 μm) (Buehler, Lake Bluff, IL).

Before thinning the cylindrical discs to the desired 1.0 mm, samples were first embedded in dental composite resin. The purpose of the embedding was to prevent leaks by increasing the sample surface area available for silicone sealant. The edges of the cylindrical discs were acid etched for 15 s using 34% phosphoric acid gel (Patterson Dental, St. Paul, MN), then washed with water for 30 s. Following the manufacturer's protocol (Kuraray America, Inc., New York, NY), CLEARFIL SE BOND primer was applied to the edges of the cylindrical disc, and then air-dried for 15 s. Then, CLEARFIL SE BOND bonding agent was gently applied to the edges of the cylindrical disc, and was photocured for 10 s under blue light (Discus Dental, Culver City, CA). The cylindrical disc was then placed concentrically in a metal washer of inner diameter 13.75 mm, CLEARFIL MAJESTY Flow flowable composite resin (Kuraray America, Inc., New York, NY) was applied between the cylindrical disc and metal washer, and was photocured for an additional 1 min 30 s. Finally,

the embedded cylindrical discs, now of diameter 13.75 mm, were thinned to 1.0 mm using water-cooled abrasive grit. For dentin samples, dentin was removed from the pulpal side of the tooth; thus, the dentin disc was taken as close as possible to the buccal side of the tooth.

For dentin samples, both sides of the disc were acid etched for an additional 30 s then washed with water for 1 min. This step was performed to expose the dentinal tubules, removing the "smear layer" formed by machination (*61*).

3.3 – One-way diffusion chamber

A one-way diffusion chamber was developed to yield a reproducible, scalable setup for running diffusion experiments in parallel. Holes of diameter 6.06 mm were drilled into 15-mL conical tube caps (BD Biosciences, Franklin Lakes, NJ) using a trephine drill (outer diameter 5.81 mm) (Henry Schein, Melville, NY). The embedded cylindrical discs were concentrically inside the conical tube cap, such that the enamel or dentin sample (~7 mm) completely covered the hole (6.06 mm). For dentin samples, the buccal side was placed face-down. To prevent leaks, silicone sealant (Dow Corning, Midland, MI) was applied at the interface between the conical tube cap and embedded cylindrical disc, and the system was left to cure for 24 hr. A schematic of the individual one-way diffusion chamber is shown in Figure 3.

To scale up the one-way diffusion chamber, the top portions of the 15-mL conical tubes were cut using a separating disc and hot-glued to the surface of a plastic containing many small ports, aligned above the wells of a 6-well plate (Greiner Bio-One, Monroe, NC). Thus, up to six diffusion experiments could be run in parallel (Figure 4). This "parallel

diffusion chamber" allowed for easy parallel access to the individual diffusion chambers. The ports allowed easy accessibility for pipetting aliquots without disturbing the diffusion during the diffusion experiment.

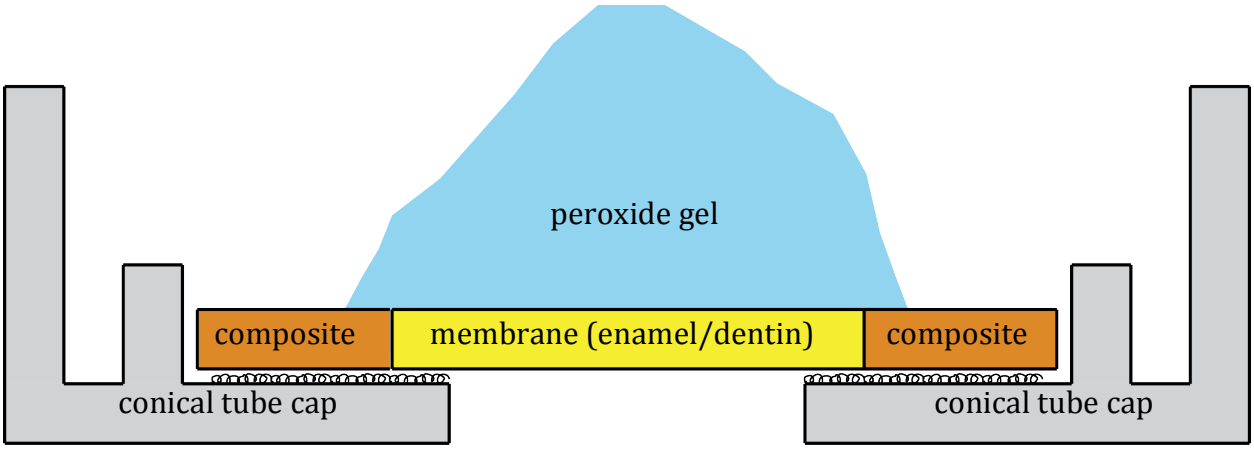

Figure 3. Schematic cross-section of individual one-way diffusion chamber.

3.4 – Diffusion experiment

Before starting diffusion, the individual diffusion chambers were first plasma etched for 1 min to improve the wettability of the conical tube cap plastic (Harrick, Ithaca, NY). The wells of the 6-well plate were filled with 5 mL deionized water, serving as the reservoir or "infinite sink." A 0.4 mL aliquot of DayWhite amorphous calcium phosphate 7.5% hydrogen peroxide gel (Discus Dental, Culver City, CA) was applied on the enamel or dentin surface facing the inside of the conical tube cap, serving as the "infinite source." Diffusion chambers were then screwed onto the conical tube tops and the parallel diffusion chamber was gently placed on top of the 6-well plate. The 6-well plate was pre-equilibrated to the

desired temperature. Each individual diffusion chamber made contact with water, positioned about 1 – 2 mm below the water surface (Figure 4).

Four degree Celsius samples were placed in a 4° C refrigerator. Room temperature (25 °C) samples were left at room temperature. Thirty-seven degree Celsius samples were placed in a 37° C humidified incubator. The system was allowed to reach steady-state for 16 hr before taking time points. During this 16 hr period, Parafilm (Bemis Company, Inc., Neenah, WI) was wrapped around the entire setup to prevent evaporation.

After 16 hr (defined as time zero), the parallel diffusion chamber was removed and replaced onto a new 6-well placed with deionized water, pre-equilibrated to the desired temperature. At 15 min intervals, 50 μL aliquots were removed from each well with a micropipette (Thermo Scientific, Waltham, MA) and placed in a 96-well plate (Greiner Bio-One, Monroe, NC) for later analysis. To prevent gradual loss of water after many time points, 50 μL aliquots of deionized water were subsequently added to the reservoir, replenishing the 5 mL volume. Upon replenishing the reservoir, each well underwent gentle pipetting up and down to ensure a well-mixed environment. Time points were taken for 2 hr (eight points per sample).

3.5 – Peroxide quantification

At the end of each 2 hr diffusion experiment, the concentration of hydrogen peroxide was quantified using a colorimetric quantitative hydrogen peroxide assay kit (National Diagnostics, Atlanta, GA). The assay is based on ferrous iron oxidation in the presence of xylenol orange (*62*). Using a 96-well plate, 90 μL of assay working reagent were

added to 10 μL of sample. The 96-well plate was then covered with Parafilm to prevent oxidation by air. After 30 min incubation at room temperature, the absorbance was measured at 560 nm (referenced at 700 nm) using a microplate reader (Tecan Group Ltd., Männedorf, Switzerland).

Hydrogen peroxide standards were prepared by performing serial dilutions from stock 30% hydrogen peroxide. Peroxide standard concentrations ranged from 50 ng/mL (the detection limit of the assay) to 2,000 ng/mL (the upper limit of the linear portion of a Beer's Law plot), plus a zero concentration corresponding to deionized water. The absorbance for each standard was measured along with the samples. A standard curve (or Beer's Law plot) was constructed and used to back out sample concentrations using measured absorbance (Figure 4). Due to the time sensitivity of the assay, a new standard curve was prepared from stock 30% hydrogen peroxide solution for each diffusion experiment performed. Samples that yielded concentration signals beyond the linear region of the Beer's Law plot were diluted, and the concentration was corrected appropriately.

To ensure that the signal produced from the samples arose entirely from oxidation by hydrogen peroxide, samples were treated with 10 μL of catalase from bovine liver, 10 mg/mL, 10,000 U/mg (Sigma, Saint Louis, MO) (*63*). Catalase catalyzes the decomposition of hydrogen peroxide to water and oxygen. Any signal obtained from catalase-treated samples should be subtracted out from the original signal. However, all samples treated with catalase produced an absorbance signal corresponding to zero concentration. Thus, there was no appreciable oxidation by molecules other than hydrogen peroxide, and the original concentration signal produced can be entirely attributed to hydrogen peroxide.

Treatment with catalase was discontinued once it became apparent that catalase-treated samples from all time points and for all temperatures yielded zero concentration.

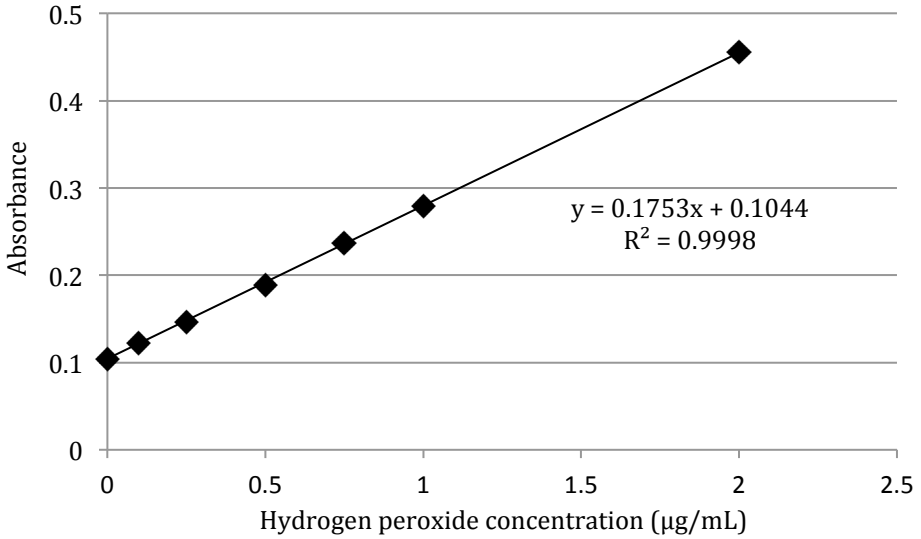

Figure 4. A typical standard curve. Absorbance axis represents difference between absorbance at 560 nm and reference absorbance at 700 nm.

Part 4 – Results

4.1 – Diffusivity of hydrogen peroxide in bovine enamel and dentin

Using the steady-state solution with reaction (and the previously obtained rate constant k of 10^{-4} s^{-1} (*60*)), the diffusivity of hydrogen peroxide at 25 °C was determined to be $5.83\times10^{-8} \pm 0.50\times10^{-8}$ cm^2/s for enamel and $1.47\times10^{-7} \pm 0.30\times10^{-7}$ cm^2/s for dentin. Comparisons between measured steady-state flux and calculated diffusivity of enamel and dentin are shown in Figure 5. Performing a Student's t-test (details given in Appendix III.1), there are statistically significant differences in both mean steady-state flux ($p < 0.05$) and mean diffusivity ($p < 0.01$) between enamel and dentin.

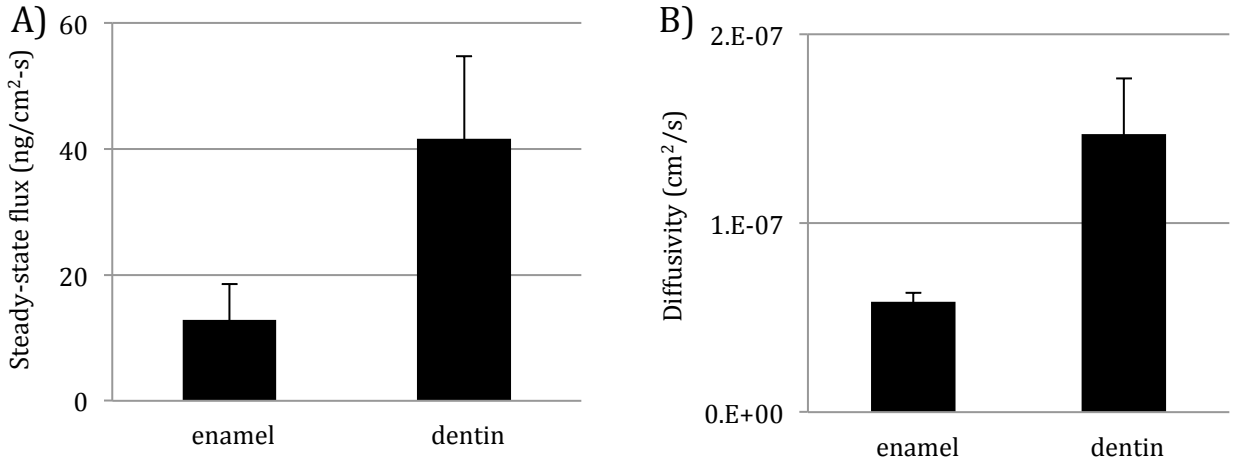

Figure 5. A) Steady-state flux of 7.5% hydrogen peroxide through bovine enamel and dentin at 25 °C. For enamel, n = 5. For dentin, n = 4. B) Calculated diffusivity of hydrogen peroxide through enamel and dentin at 25 °C. For enamel, n = 5. For dentin, n = 4.

4.2 – Temperature dependence of hydrogen peroxide diffusivity in bovine enamel

The cumulative mass diffused through enamel discs at steady-state as a function of time at various temperatures is shown in Figure 6. For each temperature, the corresponding steady-state flux and calculated diffusivity for each temperature are shown in Figure 7. The diffusivities calculated at different temperatures were determined using a rate constant k of 10^{-4} s^{-1} and a reaction temperature coefficient Q_{10} of 2. Performing a one-way analysis of variance (ANOVA) (details given in Appendix III.2), there are statistically significant differences in both mean steady-state flux ($p < 0.001$) and mean diffusivity ($p < 10^{-8}$) across the three temperature groups. Performing a Tukey's honestly significant difference (HSD) test (details given in Appendix III.3), there are statistically significant differences in mean diffusivity ($p < 0.001$) between all pairs of temperature groups; for mean steady-state flux, there are statistically significant differences between 4 °C and 37 °C groups ($p < 0.001$) and between 25 °C and 37 °C groups ($p < 0.05$), but not between 4 °C and 25 °C groups ($p < 0.1$).

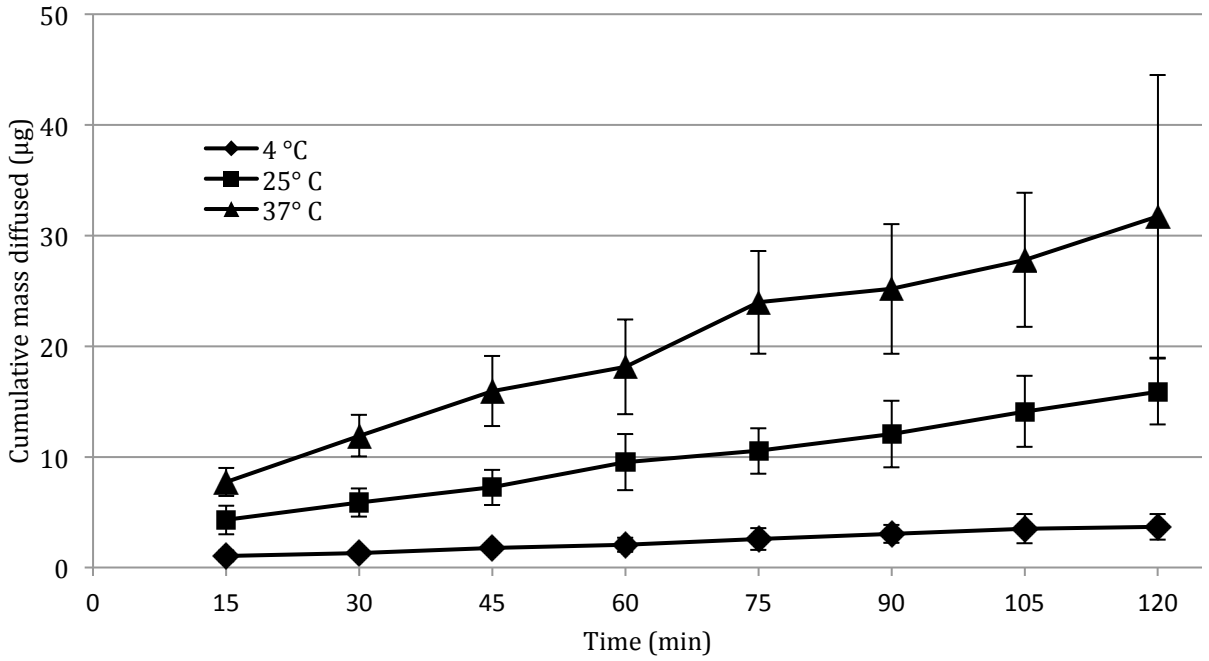

Figure 6. Steady-state diffusion of 7.5% hydrogen peroxide through bovine enamel over time at various temperatures. Time zero represents 16 hours after exposure. For 4 °C, slope = 27.0 ng/min, R^2 = 0.991. For 25 °C, slope = 109.5 ng/min, R^2 = 0.995. For 37 °C, slope = 223.1 ng/min, R^2 = 0.987. For each temperature at each time point, n = 5.

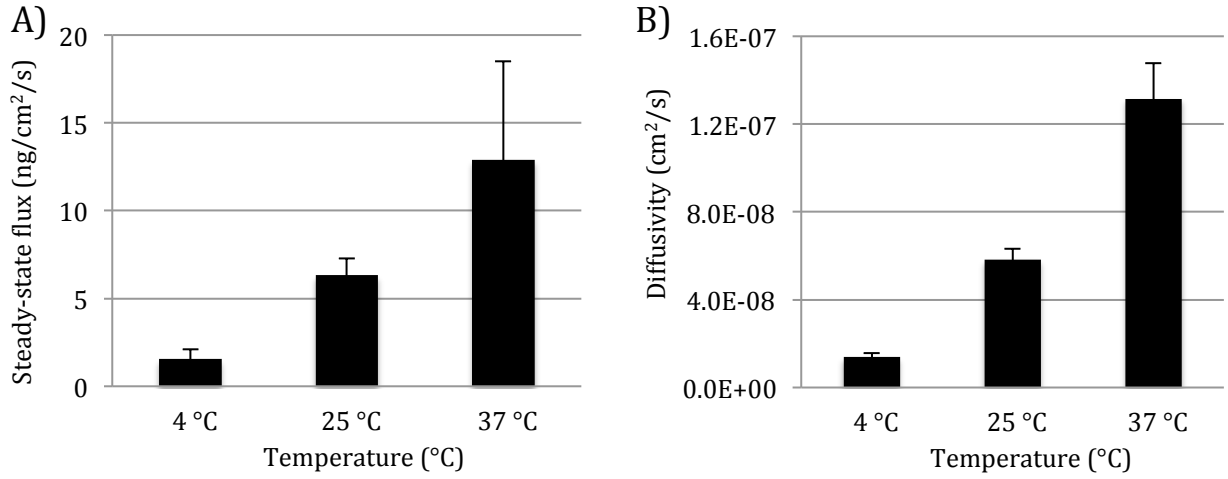

Figure 7. A) Steady-state flux of 7.5% hydrogen peroxide through bovine enamel at various temperatures. For each temperature, n = 5. B) Calculated diffusivity of hydrogen peroxide through bovine enamel at various temperatures. For each temperature, n = 5.

Linear regression analysis of an Arrhenius plot of $1/T$ versus $\ln(D/[\mathrm{cm}^2/\mathrm{s}])$ provides the thermal activation properties of hydrogen peroxide diffusion through enamel (Figure 8). The pre-exponential factor D_0 was determined to be 17.55 ± 9.65 cm²/s, and the activation energy E_a was determined to be 48.30 ± 1.34 kJ/mol, corresponding to a temperature coefficient Q_{10} of 1.95 ± 0.00.

A)

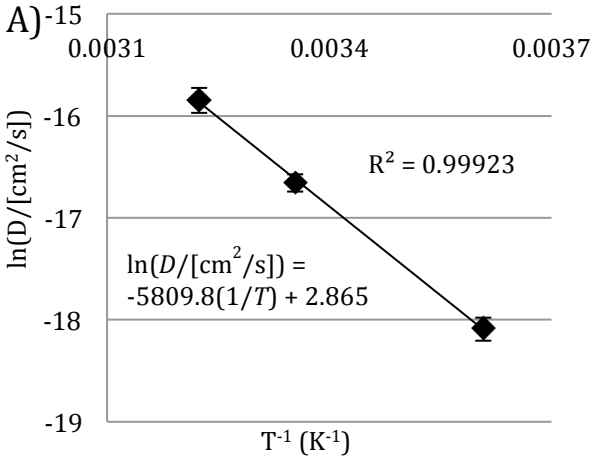

B)

$$D = D_0 \exp\left(-\frac{E_a}{RT}\right) \rightarrow \ln D = \ln D_0 - \frac{E_a}{R}\left(\frac{1}{T}\right)$$

C)

D_0 (cm²/s)	E_a (kJ/mol)	Q_{10}
17.55 ± 9.65	48.30 ± 1.34	1.95 ± 0.00

Figure 8. A) Arrhenius plot of diffusivities at various temperatures. For each temperature, n = 5. B) Linear transform of the Arrhenius equation to determine thermal activation parameters. C) Thermal activation parameters for hydrogen peroxide in enamel. Reported Q_{10} is an average of three pair-wise combinations of temperatures (4 °C, 25 °C, 37 °C).

Part 5 – Discussion

5.1 – Validity of the conservation of species equation

Experimental design, theoretical calculations, and analysis of preliminary results provide validation of both the boundary conditions applied and simplifications made to the conservation of species equation.

5.1.1 – Validity of boundary conditions

The boundary conditions are an infinite source and infinite sink on either side of the membrane. While—strictly speaking—this is known to not be true, simple calculations show that these are good approximations.

Infinite source:

A simple calculation shows that the concentration of hydrogen peroxide at the "infinite source" side of the membrane remains very close to c_0, even after 18 hours (the total time of the experiment, including the time it takes to reach steady-state). Using the largest value of steady-state flux experimentally observed, the concentration of the "source" after 18 hours is:

$$\frac{c_0 V_{\text{gel}} - JA\Delta t}{V_{\text{gel}}} \approx 0.988 c_0$$

Thus, even assuming a "worst-case" scenario in which peroxide diffuses maximally, the concentration of the source remains very close to c_0 for the duration of the experiment.

Infinite sink:

To test the validity of the "infinite sink" condition, a similar calculation is made; however, since the sink water is changed once the measurements begin, the total time is 2 hours. Using the largest value of steady-state flux experimentally observed, the concentration of the "sink" after 2 hours is:

$$\frac{JA\Delta t}{V_{\text{sink}}} \approx 0.0001 c_0$$

The maximum sink concentration is only about one-hundredth of a percent of the source concentration c_0. This is a fold-difference of four orders of magnitude. Thus, the sink concentration remains close to zero, relative to the source concentration.

5.1.2 – Validity of simplifications

The following simplifications were made to the conservation of species equation:

- One-dimensional diffusion
- No convection
- Constant diffusivity
- Pseudo-first order, homogeneous consumption reaction

One-dimensional diffusion:

By the design of the one-way diffusion chamber, there should be no radial concentration gradients, leaving only the concentration gradient through the thickness of the membrane. Furthermore, the characteristic radial length (radius or diameter) is much larger than the characteristic length through the membrane (thickness), so any small radial concentration gradients will not have appreciable effects in diffusion.

No convection:

By experimental design, the process takes place in stagnant water and thus there is no convection. Furthermore, no attempt is made to disturb the diffusion experiment.

Constant diffusivity:

By experimental design, the thicknesses of the membranes are small (~1 mm). Also, membrane sections were taken orthogonal to the enamel rods (enamel) or dentinal tubules (dentin), removing any effects of anisotropy. However, it is not feasible to experimentally show that diffusivity is constant throughout the thickness, so this remains an assumption.

Pseudo-first order, homogeneous consumption reaction:

A pseudo-first order reaction assumes that the concentration of reactants other than peroxide (i.e. stain molecules) remains constant. Since other reactions (like spontaneous peroxide degradation) can occur as well, the value for k captures effects other than irreversible staining. Thus, the reaction kinetics remains an assumption, as it is not experimentally feasible to measure stain molecule concentration within the tooth or to differentiate among various reactions.

5.1.3 – Validity of steady-state approximation

That the experimental diffusion process reaches steady-state within 16 hours is a good approximation for two reasons. Firstly, after 16 hours, experimentally measured concentrations increase linearly over time ($R^2 \approx 0.99$), suggesting that concentrations are not changing after 16 hours. Furthermore, the calculated flux was not significantly different than that taken after 48 hours instead of 16 hours, again suggesting that concentrations are not changing after 16 hours. Secondly, a theoretical calculation from Sagiv *et al*. shows that steady-state should be reached within 12 hours (*64*).

Preliminary results also validate that the steady-state model fits as well as the time-dependent model. Diffusivity values determined from the time-dependent and steady-state experiments match well when using solutions with reaction: the discrepancy between calculated diffusivities at 25 °C is less than 1.5-fold.

5.2 – Inability to ignore reaction

Both the time-dependent and steady-state solutions are much simpler without reaction (see section 2.4), so it would be beneficial to be able to use solutions without reaction to determine diffusivity values. However, preliminary results show that diffusivity values determined from the time-dependent and steady-state experiments do not match when using solutions without reaction (>5-fold difference at 25 °C). In contrast, diffusivity values determined from the time-dependent and steady-state experiments match well when using solutions with reaction (see section 5.3). Since the effect of reaction differs between time-dependent and steady-state solutions, this discrepancy between calculated diffusivities using solutions without reaction suggests that reaction cannot be ignored.

A calculation of the Thiele modulus (see section 5.6) suggests that reaction occurs quickly relative to diffusion, further suggesting that reaction cannot be ignored.

Note that the effect of reaction can be reduced by sufficiently reducing the membrane thickness; however, size constraints of the bovine teeth and the brittleness of enamel prevent thinning of the membrane to the degree that the effect of reaction becomes negligible. Thus, reaction cannot be ignored experimentally.

5.3 – Validity of rate constant used

The previously established rate constant k of 10^{-4} s^{-1} was used (*60*). To validate this value, results from a non-steady-state diffusion experiment with enamel (see Figure 9A) was fitted to the time-dependent solution with reaction. Fitting both parameters (D and k)

to the solution using nonlinear least-squares regression (see Appendix II.2), the value of D was determined to be 5.67×10^{-8} cm^2/s and the corresponding value of k was determined to be 2.12×10^{-4} s^{-1} ($R^2 = 0.9921$).

Similarly, a fit to the results from the non-steady-state diffusion experiment with dentin by Hannig *et al*. (*58*) using nonlinear least-squares regression yields $D = 3.09\times10^{-7}$ and $k = 8.71\times10^{-4}$ s^{-1} ($R^2 = 0.9984$) (see Figure 9B).

For both the non-steady-state experiments here and previous non-steady-state experiments, the calculated values for k are close to the value used (10^{-4} s^{-1}). Furthermore, the corresponding calculated values of D are also close to those calculated from the steady-state experiment. Thus, the rate constant used is accurate. Furthermore, the mass transport parameters obtained using the non-steady-state experiment closely match those of the steady-state experiment, confirming the validity of using the steady-state solution.

5.4 – Justification for focus on enamel

The focus of this study is on the transport properties of hydrogen peroxide through enamel rather than dentin. Figure 1 shows that diffusivity of hydrogen peroxide is more than 2.5 times greater in enamel than dentin. Thus, diffusion through enamel is the rate-limiting step for clinical applications.

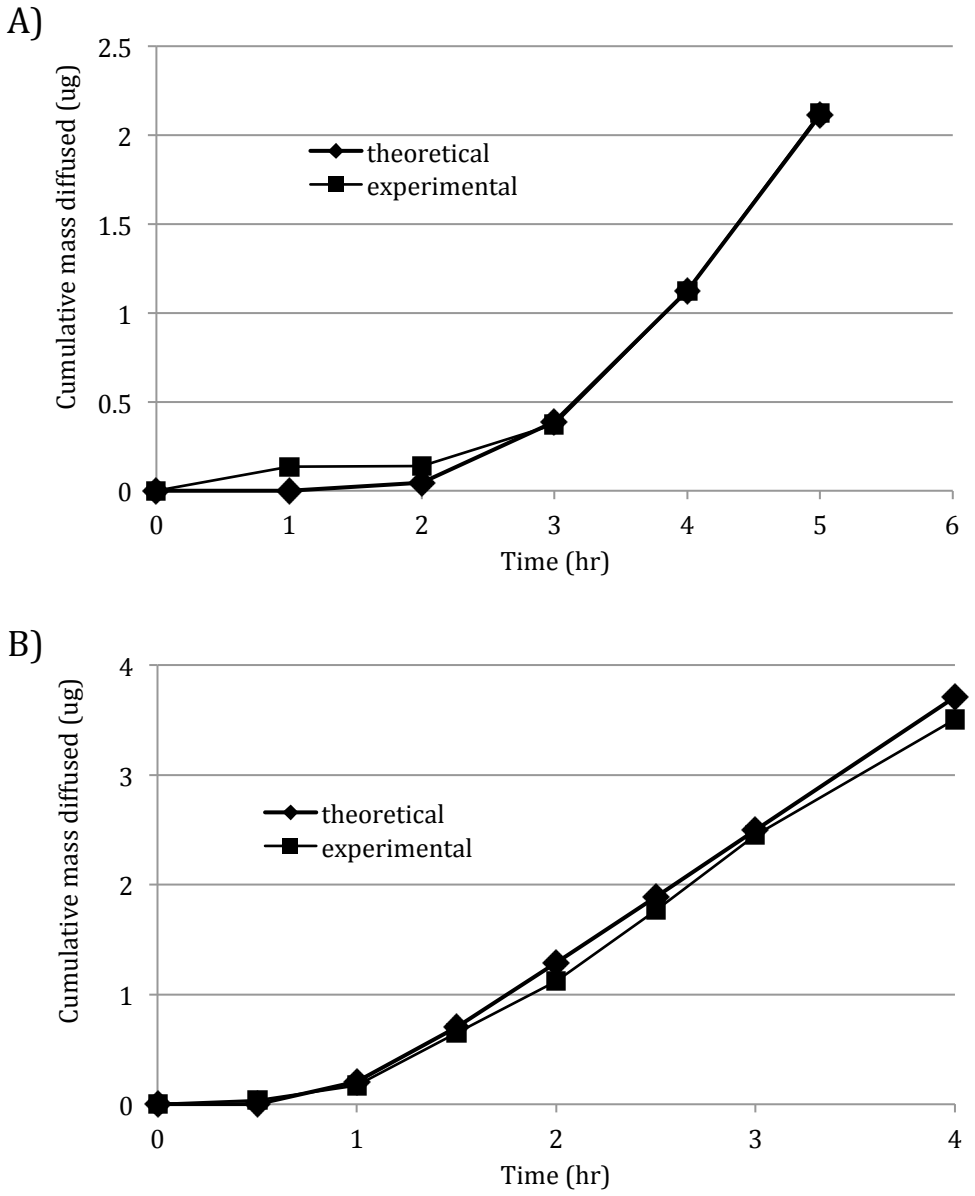

Figure 9. A) Typical results of non-steady-state diffusion of 7.5% hydrogen peroxide through bovine enamel, along with theoretical calculations for cumulative mass diffused determined by nonlinear least-squares regression $(\boldsymbol{D = 5.67\times 10^{-8}}$ cm^2/s, $\boldsymbol{k = 2.12\times 10^{-4}}$ s^{-1}, $\boldsymbol{R^2 = 0.9921})$. B) Results of Hannig *et al*. (*58*), along with theoretical calculations for cumulative mass diffused determined by nonlinear least-squares regression ($\boldsymbol{D = 3.09\times 10^{-7}}$ cm^2/s, $\boldsymbol{k = 8.71\times 10^{-4}}$ s^{-1}, $\boldsymbol{R^2 = 0.9984}$).

5.5 – Effects of altering reaction parameters k and reaction-Q_{10}

Note that activation energy E_a and temperature coefficient Q_{10} values are intrinsically linked. Given E_a, Q_{10} can be determined explicitly using the formula:

$$Q_{10} = \exp\left(\frac{10E_a}{RT_1T_2}\right)$$

Clearly, increasing E_a results in increasing Q_{10}. Strictly speaking, E_a and Q_{10} are functions of temperature; however, for temperatures near physiological values (including the experimental temperature range, 4 – 37 °C), both E_a and Q_{10} remain relatively independent of temperature (within ~5% difference).

For the same experimental data, increasing k results in an increased calculated D. This is because the diffusion must increase to compensate for increased consumption along the diffusion path. This effect is more pronounced at low temperatures than for high temperatures. Thus, calculated D for various temperatures are closer together, resulting in decreased diffusion-Q_{10}. Consequently, diffusion-E_a also decreases as k increases.

The above effects are appreciable for reaction-Q_{10} = 1. For reaction-Q_{10} = 2, changes in diffusion-Q_{10} and diffusion-E_a with increasing k are negligible. These effects are summarized in Table 2. Theoretically, diffusion-E_a (and diffusion-Q_{10}) should be independent of reaction rate k. Thus, that choosing reaction-Q_{10} = 2 results in stable diffusion-E_a (and diffusion-Q_{10}) suggests that the true value of reaction-Q_{10} is indeed close to 2.

Table 2. Effects of increasing k for two values of reaction-Q_{10}.

Reaction-Q_{10} = 1			**Reaction-Q_{10} = 2**		
Parameter	**Change**	**Effect size**	**Parameter**	**Change**	**Effect size**
Diffusivity	Increase	Appreciable	Diffusivity	Increase	Appreciable
Diffusion-Q_{10}	Decrease	Appreciable	Diffusion-Q_{10}	Decrease	Negligible
Diffusion-E_a	Decrease	Appreciable	Diffusion-E_a	Decrease	Negligible

5.6 – Thiele modulus

The Thiele modulus is a dimensionless quantity used to relate the relative rates of diffusion and reaction for transport in porous media (*65*). The Thiele modulus ϕ_n is determined using the relation (*66*):

$$\phi_n^2 = \frac{\text{reaction rate}}{\text{diffusion rate}} = \frac{\text{characteristic diffusion time scale}}{\text{characteristic reaction time scale}} = \frac{L^2/D}{1/kc^{n-1}},$$

where L is the membrane thickness, D is diffusivity, k is rate constant, c is concentration, and n is the reaction order. Since the reaction here is pseudo-first order, $n = 1$. When $\phi_n^2 \gg 1$, the reaction occurs quickly relative to diffusion, thus the process is diffusion-limited. When $\phi_n^2 \ll 1$, reaction occurs slowly relative to diffusion, thus the process is reaction-limited. When $\phi_n^2 \sim 1$, neither reaction nor diffusion dominate transport.

Using values determined for enamel at 25 °C, $\phi_1^2 = 17.14 \pm 1.45$. For dentin, $\phi_1^2 = 6.80 \pm 1.37$. Thus, for both enamel and dentin, reaction occurs quickly compared to diffusion, thus the transport process is diffusion-limited. As expected, ϕ_1^2 is larger for enamel than dentin because D is smaller but k is the same.

Note that since values for reaction-Q_{10} and diffusion-Q_{10} are similar, changes in D and k with temperature will effectively cancel in the formula for ϕ_1. Thus, ϕ_1 does not change significantly with temperature.

5.7 – Comparisons of experimental data to existing experimental data

While the diffusivity and thermal activation energy of hydrogen peroxide in enamel is determined here for the first time, comparisons can be made to other diffusates in similar porous media (Table 3). Note that quantitative comparisons of diffusivities have limited relevance across different diffusion platforms and experimental setups. For example, diffusivity of water is traditionally determined using liquid scintillation counting of radioactive tritiated water molecules at concentrations around nine orders of magnitude lower than the peroxide concentrations used here (*67*). Since diffusivity fluctuates with concentration, these gross differences may render quantitative cross-experiment comparisons unhelpful.

The determined diffusivity and activation energy of hydrogen peroxide in enamel are larger than those of water in enamel by Burke *et al* (*67*). Since hydrogen peroxide is larger than water, diffusivity is expected to be smaller. This discrepancy is likely due to the assumptions made in calculating diffusivity. For example, the diaphragm cell method used by Burke *et al.* is based on a different diffusate "standard" of known diffusivity; thus, its accuracy is fundamentally limited by the accuracy of the diffusate standard.

Compared to the results of Van der Graaf *et al*. concerning tritiated water diffusion through dentin, the determined peroxide diffusivity in enamel is significantly lower and the activation energy is higher (*68, 69*). This is consistent with expected results, as large dentinal tubules result in higher dentin diffusivity, and the more constricting pores in enamel are associated with higher activation energy. A similar argument holds for the

results of diffusion of Fernández-Seara *et al*. for water in bone, as bone is more porous than enamel (*70*).

Table 3. Comparisons of results to existing experimental apparent diffusivities and activation energies for various diffusates in various porous media.

Diffusate	**Medium**	D_a **at 25 °C** (10^8 **cm²/s)**	E_a **(kJ/mol)**	**Reference**
Hydrogen peroxide	Bovine incisor enamel	5.83 ± 0.50	48.30 ± 1.34	This study
Water	Human incisor enamel	0.56 – 1.71	22 – 42	(*67*)
Water	Canine enamel	0.35 – 0.54	46 – 61	(*67*)
Water	Human molar dentin	174 ± 43	29.5 ± 2.2	(*68, 69*)
Water	Rabbit cortical bone	35.6 ± 7.8	26.6 – 26.8	(*70*)
Sodium	Human molar enamel	1.98 – 7.44	21 – 26	(*71*)
Fluoride	Human premolar enamel	0.46 ± 0.16	N/A	(*72*)
SiF_6	Human premolar enamel	0.26 ± 0.12	N/A	(*72*)
PO_3F	Human premolar enamel	0.17 ± 0.07	N/A	(*72*)

5.8 – SEM analysis

Scanning electron microscope (SEM) images were taken to ensure that there were no microcracks present in dentin or enamel caused by machination (FEI Company, Hillsboro, OR). Characteristic SEM images are shown in Figure 9. Any samples with cracks were not used for diffusion experiments. Furthermore, SEM images of the interface between enamel or dentin and the composite resin show tight seals without gaps, ensuring that leakage did not occur through the interface during diffusion experiments (Figure 9C,D).

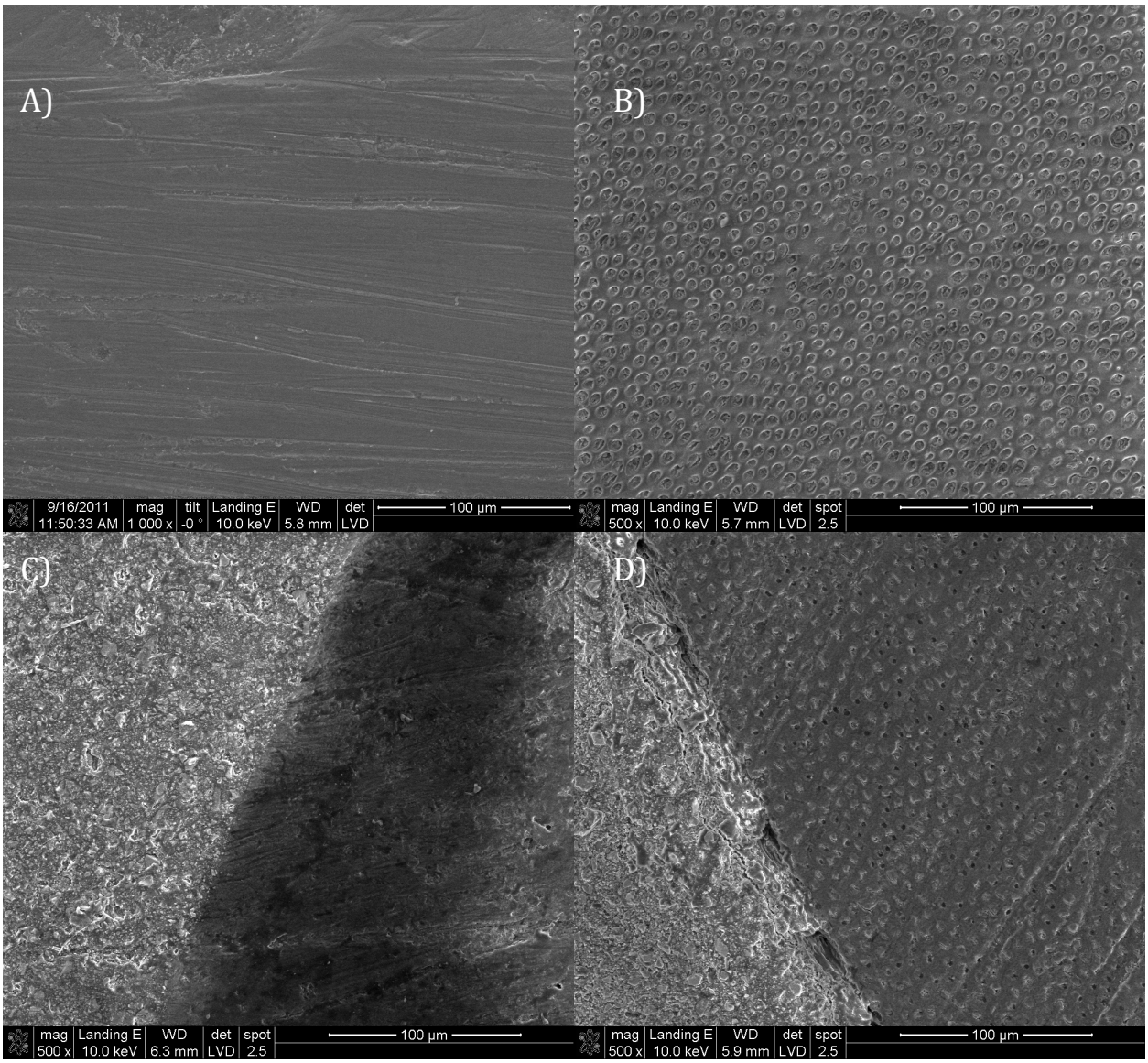

Figure 10. A) Enamel surface (magnification 1000x). B) Dentin surface (enamel side), revealing exposed dentinal tubules (magnification 500x). C) Interface between composite resin (left) and enamel (right) (magnification 500x). D) Interface between composite resin (left) and dentin (right) (magnification 500x).

Part 6 – Conclusions and future direction

6.1 – Conclusions

Based on the findings presented here, the following conclusions can be made:

1. The experimental setup (either time-dependent or steady-state), fitted to the mathematical model, is sufficient to back out physical mass transport parameters for multiple platforms involving diffusion through porous media, with or without irreversible reaction.
2. Hydrogen peroxide transport occurs significantly faster through bovine dentin than enamel.
3. Hydrogen peroxide transport in bovine enamel is a thermally activated process.
4. Hydrogen peroxide transport in both bovine enamel and dentin is diffusion-limited.

6.2 – Optimizing tooth whitening using finite element analysis models

Now that the physical transport properties through teeth have been determined, whole tooth models can be used to optimizing tooth whitening conditions like application time and renewal time. Such a model requires numerical finite element analysis tools such as COMSOL Multiphysics, similar to Satish *et al*. (*60*). Using the mass transport and thermal activation properties determined here, the transport properties at each point in a three-dimensional tooth model can be calculated, and the three-dimensional hydrogen peroxide concentration profile over time can be simulated. Using clinically determined parameters

like a threshold level of peroxide penetration into the pulp chamber, the model can quantitatively optimize tooth whitening parameters like application time and renewal time, which currently remain empirical (*13*).

Numerical, three-dimensional analysis allows for loosening of certain assumptions and inclusion of additional contributions to mass transport appropriate to mimic the *in vivo* environment. The boundary conditions of the problem should be loosened to account for a finite amount of hydrogen peroxide. Additional contributions to mass transport should also be considered, including: the change in dentin diffusivity with radial distance from the pulp chamber; hydrostatic pressure contributions from the fluid-filled dentinal tubules and pulp chamber; systemic clearance of peroxide entering the pulp chamber.

Since this model is designed to mimic the *in vivo* environment, experimental parameters must be confined within clinical relevance. Note that this is in contrast with the current studies aimed at determining the physical parameters of peroxide transport in teeth, which do not require confinement to clinical or even physiological conditions.

6.3 – Controlling diffusion

Since hydrogen peroxide diffusion is found to occur slowly compared to reaction, it makes sense to primarily target diffusion for controlling mass transport. Ideally, diffusion should occur relatively quickly through enamel, since dentin is the primary target for bleaching, and should slow or stop just before reaching the pulp chamber, in order to prevent tooth sensitivity and risk of pulpal damage. Thus, methods aimed at controlling

diffusion should seek to increase diffusion toward the enamel side of the tooth, and slow, stop, or reverse diffusion toward the pulpal side.

6.3.1 – Heating and cooling

One proposed method to control diffusion is to heat the front side of the tooth and simultaneously cool the back of the tooth during in-office whitening treatment. Heating can be achieved using a lamp or laser on the surface of the teeth with peroxide gel. Cooling can be achieved by flowing cold water across the back of the teeth. Since this study has found that diffusion occurs faster for high temperatures and slower for low temperatures, simultaneous heating and cooling could improve whitening efficacy while reducing risk of side-effects, and may results in shorter application times.

Mathematical modeling of simultaneous heating and cooling during whitening requires a whole tooth model that mimics *in vivo* conditions (see 6.2). Such a model could apply heat transfer theory to a three-dimensional tooth model to determine the temperature of the tooth at each point when applying simultaneous heating and cooling. Simulations of the peroxide concentration profile over time can be combined with clinically determined safety parameters to optimize a simultaneous heating and cooling method to increase whitening efficacy while reducing risk of tooth sensitivity or damage.

Since this model is designed to mimic the *in vivo* environment, the heating and cooling temperatures must be confined within clinical safety. Laser application has shown to increase the surface temperature of the tooth by 11.6 °C, with the presence of the peroxide gel (*73*). Lasers application also increases the pulpal temperature by about 7 °C

for teeth with the presence of peroxide gel (*73*); however, conservative studies suggest that the clinically safe threshold increase in pulpal temperature is 5.5 °C (*31*). On the opposite end of the spectrum, one study determined the pain threshold for cold sensitivity in teeth to be 14.2 °C (*74*). While existing studies provide preliminary model parameters, further clinical studies may be required to better determine pain and safety threshold temperature levels for simultaneous heating and cooling.

6.3.2 – Iontophoresis

Another proposed method to control diffusion is to drive diffusion using iontophoresis. Traditionally, iontophoresis is a non-invasive technique to deliver drugs transdermally. The device applies an electric potential to a drug-filled patch contacting the skin, causing the charged drug molecules to penetrate into the skin. For tooth whitening applications, the same process may be applied to a peroxide-filled patch contacting the skin. Peroxide diffusion may increase or decrease via molecular interactions with ions being driven by iontophoresis, which may be introduced in the whitening formulation or already present in the saline-saturated teeth. For example, if an applied positive potential increases diffusion, an applied negative potential may reduce diffusion or even reverse its direction. Thus, diffusion may be increased until significant peroxide penetration into the pulp chamber occurs, then decreased or reversed to prevent excessive penetration. Time-time dependent transport models with a tunable correction representing the effect of iontophoresis can be used to determine an appropriate time delay before slowing or reversing diffusion.

Appendix I – Separation of variables

The following initial-boundary-value problem will be solved using separation of variables:

$$\begin{cases} \dfrac{\partial c}{\partial t} = D\dfrac{\partial^2 c}{\partial x^2} \\ c(x=0,t) = c_0 \\ c(x=L,t) = 0 \\ c(x,t=0) = 0 \end{cases}$$

First, the solution can be separated into two terms:

$c(x,t) = c_1(x) + c_2(x,t)$,

where c_1 solves the corresponding homogeneous differential equation with the non-homogeneous boundary conditions and c_2 solves the non-homogeneous differential equation with corresponding homogeneous boundary conditions.

In other words,

$$\begin{cases} 0 = D\dfrac{d^2 c_1}{dx^2} \\ c_1(x=0) = c_0 \\ c_1(x=L) = 0 \end{cases}$$

and

$$\begin{cases} \dfrac{\partial c_2}{\partial t} = D\dfrac{\partial^2 c_2}{\partial x^2} \\ c_2(x=0,t) = 0 \\ c_2(x=L,t) = 0 \\ c_2(x,t=0) = 0 \end{cases}$$

c_1 can be easily determined by integrating both sides of the equation twice:

$c_1 = k_1 x + k_2$, where k_1 and k_2 are constants of integration.

Applying the boundary conditions,

$$c_1 = c_0 - \frac{c_0}{L}x = c_0\left(1 - \frac{x}{L}\right)$$

Assume that c_2 takes the form:

$$c_2(x,t) = X(x)T(t)$$

Substituting back into the partial differential equation,

$$X(x)T'(t) = DX''(x)T(t)$$

Rearranging,

$$\frac{T'(t)}{DT(t)} = \frac{X''(x)}{X(x)}$$

Since the left-hand side of the equation is only a function of *t*, and the right-hand side is only a function of *x*, then both sides must be equal to a constant, defined as -λ. Then,

$$T' = -\lambda DT$$

$$X'' = -\lambda X$$

The solution for T is an exponential:

$T = T_0 \exp(-\lambda Dt)$, where T_0 is an arbitrary constant.

Since the concentration cannot indefinitely increase in time, T must decay exponentially in time. Hence, λ must be positive. Then,

$X = K_1 \cos\left(\sqrt{\lambda}x\right) + K_2 \sin\left(\sqrt{\lambda}x\right)$, where K_1 and K_2 are arbitrary constants.

Applying the first boundary condition, since T is not identically equal to zero,

$X(0) = 0$, so $K_1 = 0$

Applying the second boundary condition, since T is not identically equal to zero,

$$X(L) = \sin\left(\sqrt{\lambda}L\right) = 0$$

Thus, λ is an eigenvalue of X and can take on an infinite number of values λ_n, corresponding to eigenfunctions X_n, where n is a positive integer:

$$\sin\left(\sqrt{\lambda}L\right) = 0$$

$$\sqrt{\lambda_n}L = n\pi$$

$$\lambda_n = \left(\frac{n\pi}{L}\right)^2$$

$$X_n = \sin\left(\sqrt{\lambda_n}x\right) = \sin\left(\frac{n\pi x}{L}\right)$$

The sum of solutions to the differential equation which satisfy the boundary conditions also satisfies the differential equation and boundary conditions. Thus, the solution to c_2 is:

$$c_2 = \sum_{n=1}^{\infty} A_n \sin\left(\frac{n\pi x}{L}\right) \exp\left[-D\left(\frac{n\pi}{L}\right)^2 t\right],$$

where A_n are constants determined by the initial conditions.

Thus,

$$c(x,t) = c_0\left(1 - \frac{x}{L}\right) + \sum_{n=1}^{\infty} A_n \sin\left(\frac{n\pi x}{L}\right) \exp\left[-D\left(\frac{n\pi}{L}\right)^2 t\right]$$

Using the initial condition,

$$c(x, t=0) = c_0\left(1 - \frac{x}{L}\right) + \sum_{n=1}^{\infty} A_n \sin\left(\frac{n\pi x}{L}\right) = 0$$

Rearranging,

$$\sum_{n=1}^{\infty} A_n \sin\left(\frac{n\pi x}{L}\right) = -c_0\left(1 - \frac{x}{L}\right)$$

The left-hand side of the equation is the Fourier sine series expansion of the right-hand side. Multiplying both sides of the equation by $\sin\left(\frac{n\pi x}{L}\right)$ and integrating from 0 to L,

$$\int_0^L \sum_{n=1}^{\infty} A_n \sin\left(\frac{n\pi x}{L}\right) \sin\left(\frac{m\pi x}{L}\right) dx = \int_0^L -c_0 \left(1 - \frac{x}{L}\right) \sin\left(\frac{m\pi x}{L}\right) dx$$

Since eigenfunctions are orthogonal, terms on the left-hand side of the equation are equal to zero for $m \neq n$. When $m = n$,

$$\int_0^L A_n \sin^2\left(\frac{n\pi x}{L}\right) dx = \int_0^L -c_0 \left(1 - \frac{x}{L}\right) \sin\left(\frac{n\pi x}{L}\right) dx$$

$$A_n = \frac{\int_0^L -c_0 \left(1 - \frac{x}{L}\right) \sin\left(\frac{n\pi x}{L}\right) dx}{\int_0^L A_n \sin^2\left(\frac{n\pi x}{L}\right) dx} = \frac{\int_0^L -c_0 \left(1 - \frac{x}{L}\right) \sin\left(\frac{n\pi x}{L}\right) dx}{\frac{L}{2}}$$

$$A_n = -c_0 \frac{2}{n\pi}$$

Thus, the final solution for c is:

$$c(x,t) = c_0 \left(1 - \frac{x}{L}\right) - c_0 \sum_{n=1}^{\infty} \frac{2}{n\pi} \sin\left(\frac{n\pi x}{L}\right) \exp\left[-D\left(\frac{n\pi}{L}\right)^2 t\right]$$

Appendix II – Annotated code for software programs

Appendix II.1 – Numerical determination of diffusivity using steady-state solution with reaction

```
#include <iostream>
#include <math.h>
using namespace std;

//Initialize universal constants
const double PI = 3.14159265;

int main (int argc, const char * argv[])
{
    //Initialize experimental parameters
    const double A = PI*pow(0.303,2); //Surface area of tooth [cm^2]
    const double C0 = 0.075; //Peroxide concentration [g/mL]
    const double Q10_k = 2; //Reaction temperature coefficient
[unitless]
    const double T0 = 25; //Room temperature [°C]
    const double k_rxn_0 = 1e-4; //Rate constant at room temperature
[s^-1]
    const int NUM_INCREMENTS = 1000000; //Number of diffusivity values
being tried
    const int NUM_SAMPLES = 19; //Number of samples
    double L[NUM_SAMPLES] =
{1.01,0.99,0.99,0.96,0.99,0.96,1.01,0.97,0.99,0.96,1,1,0.99,0.99,1,0.9
9,1.05,1.00,1.01; //Membrane thickness [mm]
    double T[NUM_SAMPLES] =
{4,4,4,4,4,25,25,25,25,25,37,37,37,37,37,25,25,25,25}; //Temperature
[°C]
    double k_rxn[NUM_SAMPLES]; //Rate constant [s^-1]
    double exp_slope[NUM_SAMPLES] =
{15.71714763,25.09969721,22.94095013,41.48301,29.64989299,98.14741955,
131.325869,91.86458479,104.7322906,121.4809234,246.1990961,335.2009106
,201.7823116,155.5428686,190.3696656,833.7927376,915.4849135,399.19462
22,730.4366914}; //Slope [ng/min]

    //Determine rate constant for each sample based on temperature
    for(int i = 0; i < NUM_SAMPLES; i++)
        k_rxn[i] = k_rxn_0*pow(Q10_k,(T[i]-T0)/10);

    //Initialize theoretical slopes
    double theor_slope[NUM_SAMPLES];
```

```
    //Initialize diffusivity constants incrementally
    double D;
    double D_lower = 1e-08;
    double D_upper = 1e-06;

    //Initialize house-keeping variables
    double diff1, diff2;
    double D_best[NUM_SAMPLES];
    double slope_best[NUM_SAMPLES];

    for(int i = 0; i < NUM_SAMPLES; i++) //For each sample
    {
        D = D_lower; //Start at lower bound
        D_best[i] = D;
        while (D <= D_upper) //For each diffusivity being tried
        {
            //Increment diffusivity
            D += D_upper/NUM_INCREMENTS;
            //Calculate theoretical slope based on diffusivity
            theor_slope[i] =
60*pow(10,9)*C0*A*sqrt(k_rxn[i]*D)/sinh(L[i]*0.1*sqrt(k_rxn[i]/D));

            if(theor_slope[i]-exp_slope[i] > 0)
                diff1 = theor_slope[i]-exp_slope[i];
            else
                diff1 = exp_slope[i]-theor_slope[i];
            if(slope_best[i]-exp_slope[i] > 0)
                diff2 = slope_best[i]-exp_slope[i];
            else
                diff2 = exp_slope[i]-slope_best[i];

            //If theoretical slope is closer to experimental slope
than the best slope
            if(diff1 < diff2)
            {
                //Update best slope and diffusivity
                slope_best[i] = theor_slope[i];
                D_best[i] = D;
            }
        }
    }

    //Display diffusivity values for each sample
    for(int i = 0; i < NUM_SAMPLES; i++)
        cout << "\n" << "D[" << i << "] = " << D_best[i];

    return 0;
}
```

Appendix II.2 – Nonlinear least-squares regression to determine diffusivity and rate constant using time-dependent solution with reaction

```
#include <iostream>
#include <math.h>
using namespace std;

//Initialize universal constants
const double PI = 3.14159265;

int main (int argc, const char * argv[])
{
    //Initialize experimental parameters
    const int NUM_POINTS = 6; //Number of time points
    double time[NUM_POINTS] = {0,3600,7200,10800,14400,18000}; //Time
points [sec]
    const double A = PI*pow(0.303,2); //Surface area of tooth [cm^2]
    const double C0 = 0.075; //Peroxide concentration [g/mL]
    const double L = 0.1; //Membrane thickness[cm]

    //Initialize experimental mass at each time point
    double exp_mass[NUM_POINTS] =
{0,134.8725734,137.3702137,373.9324258,1126.792558,2122.994212};

    //Initialize finite approximation for infinite sum
    const int N_SUM = 100;

    //Initialize parameter limits and increments
    double D_min = 1e-08;
    double D_max = 1e-06;
    double D_inc = D_max/10000;
    double k_min = 1e-5;
    double k_max = 1e-4;
    double k_inc = k_max/10000;
    double D = D_min;
    double k = k_min;

    //Initialize regression numbers
    double SS_err = 0;
    double SS_tot = 0;
    double R_squared = 0;

    //Initialize housekeeping variables
    double R_squared_best = 0;
    double k_best;
    double D_best;
```

```
    //Initialize theoretical mass array
    double theor_mass[NUM_POINTS];

    //Calculate total sum of squares
    double average = 0;
    for(int i = 0; i < NUM_POINTS; i++)
        average += exp_mass[i]/NUM_POINTS;
    for(int i = 0; i < NUM_POINTS; i++)
        SS_tot += pow(exp_mass[i]-average,2);

    while(D < D_max) //For each diffusivity
    {
        while(k <= k_max) //For each rate constant
        {
            for(int i = 0; i < NUM_POINTS; i++) //For each time point
            {
                //Calculate linear term
                theor_mass[i] = pow(10,9)*C0*A*D*time[i]/L;
                //Calculate non-linear terms
                for(int n = 1; n < N_SUM; n++)
                {
                    if(n%2 == 0)
                        theor_mass[i] +=
2*pow(10,9)*C0*D*A/L*(pow((n*PI/L),2)*D*(1+k*time[i]-exp(-
D*pow((n*PI/L),2)*time[i]-
k*time[i]))+pow(k,2)*time[i])/pow((pow((n*PI/L),2)*D+k),2);
                    else
                        theor_mass[i] -=
2*pow(10,9)*C0*D*A/L*(pow((n*PI/L),2)*D*(1+k*time[i]-exp(-
D*pow((n*PI/L),2)*time[i]-
k*time[i]))+pow(k,2)*time[i])/pow((pow((n*PI/L),2)*D+k),2);
                }
                //Calculate sum of squares of error
                SS_err += pow(exp_mass[i]-theor_mass[i],2);
            }
            //Calculate R-squared
            R_squared = 1-SS_err/SS_tot;
            //If new R-squared is greater than best R-squared
            if(R_squared > R_squared_best)
            {
                //Update best R-squared, diffusivity, and rate
constant
                R_squared_best = R_squared;
                D_best = D;
                k_best = k;
            }
            SS_err = 0; //Reset sum of squares for error
            k += k_inc; //Increment rate constant
        }
        k = k_min; //Reset rate constant
```

```
        D += D_inc; //Increment diffusivity
    }

    //Display best value of R-squared, with corresponding diffusivity
and rate constant
    cout << "R-squared = " << R_squared_best << "\nD = " << D_best <<
"\nk = " << k_best << "\n\n";

    return 0;
}
```

Appendix III – Statistical methods

Appendix III.1 – Student's *t*-test

A Student's *t*-test is a statistical hypothesis test in which the test statistic follows a Student's t distribution if the null hypothesis is accepted. The test makes the following assumptions:

- Populations follow a standard normal distribution under the null hypothesis
- Populations have equal variance
- Samples are independent

An independent two-sample *t*-test is used for equal sample sizes when the variances of the two distributions are equal. Under the null hypothesis, the means of the two samples are equal. In this case, the test statistic is:

$$t = \frac{\bar{x}_1 - \bar{x}_2}{\sqrt{\frac{s_{x_1}^2 + s_{x_2}^2}{n}}},$$

where $\bar{x}_1$ and $\bar{x}_2$ are the sample means, s_{x_1} and s_{x_1} are the sample standard deviations, and n is the sample size of each group.

The p-value is determined using a Student's t distribution. The number of degrees of freedom is $2n - 2$. Here, p-values less than 0.05 are considered statistically significant.

Appendix III.2 – One-way analysis of variance (ANOVA)

A one-way analysis of variance (ANOVA) is a statistical hypothesis test in which the test statistic follows an F-distribution under the null hypothesis. It is used to compare means of two or more samples. The test makes the following assumptions:

- Response variables are normally distributed
- Populations have equal variance
- Samples are independent

Under the null hypothesis, the means of all groups are equal. The test statistic is:

$$F = \frac{\sum_{i=1}^{k} n_i \left(\overline{Y}_i - \overline{\overline{Y}}\right)^2 / (k-1)}{\sum_{i=1}^{k} \sum_{j=1}^{n_i} \left(Y_{ij} - \overline{Y}_i\right)^2 / (N-k)},$$

where k is the number of groups, n_i is the sample size of the i^{th} group, $\overline{Y}_i$ is the mean of the i^{th} group, $\overline{\overline{Y}}$ is the overall mean, Y_{ij} is the j^{th} value in the i^{th} group, and N is the overall sample size.

The p-value is determined using an F-distribution. The number of degrees of freedom is $k - 1$ for the numerator and $N - k$ for the denominator of the F-distribution. Here, p-values less than 0.05 are considered statistically significant.

Appendix III.3 – Tukey's honestly significant difference (HSD) test

A Tukey's honestly significant difference (HSD) test is a statistical hypothesis test in which the test statistic follows a studentized range (q) distribution under the null

hypothesis. It is often used in conjunction with an ANOVA to find which means are significantly different from one another. The test makes the following assumptions:

The test makes the following assumptions:

- The observations being tested are independent
- There is equal variation across observations

Under the null hypothesis, all means being compared are equal. When the sample sizes of all groups are equal, the test statistic for each pair of groups is:

$$q = \frac{Y_A - Y_B}{\sqrt{\sum_{i=1}^{k}\sum_{j=1}^{n}\left(Y_{ij} - \bar{Y}_i\right)^2 / kn(n-1)}},$$

where Y_A is the larger of the two means being compared, Y_B is the smaller of the two means being compared, k is the number of groups, n is the sample size of each group, Y_{ij} is the j^{th} value of the i^{th} group, and $\bar{Y}_i$ is the mean of the i^{th} group.

The p-value is determined using a q distribution. The number of degrees of freedom is $k(n-1)$. Here, p-values less than 0.05 are considered statistically significant.

References

1. K. J. Laidler, The development of the Arrhenius equation. *Journal of Chemical Education* **61**, 494 (1984).
2. W. Hayduk, H. Laudie, Prediction of diffusion coefficients for nonelectrolytes in dilute aqueous solutions. *AIChE Journal* **20**, 611 (1974).
3. B. P. Luo, S. L. Clegg, T. Peter, R. Müller, P. J. Crutzen, HCl solubility and liquid diffusion in aqueous sulfuric acid under stratospheric conditions. *Geophysical research letters* **21**, 49 (1994).
4. M. Malmsten, B. Lindman, Water self-diffusion in aqueous block copolymer solutions. *Macromolecules* **25**, 5446 (1992).
5. E. H. Oelkers, Calculation of diffusion coefficients for aqueous organic species at temperatures from 0 to 350 C. *Geochimica et Cosmochimica Acta* **55**, 3515 (1991).
6. E. L. Cussler, *Diffusion: Mass transfer in fluid systems*. (Cambridge Univ Pr, 1997).
7. J. Van Brakel, P. M. Heertjes, Analysis of diffusion in macroporous media in terms of a porosity, a tortuosity and a constrictivity factor. *International Journal of Heat and Mass Transfer* **17**, 1093 (1974).
8. G. H. Dibdin, Models of diffusion/reaction in dental plaque. *Microbial Ecology in Health and Disease* **8**, 317 (1995).
9. C. H. Tonge, Development, Function and Evolution of Teeth. *Journal of the Royal Society of Medicine* **72**, 162 (1979).

10. G. Tang *et al.*, Optimization of b value in diffusion-weighted MRI for the differential diagnosis of benign and malignant vertebral fractures. *Skeletal radiology* **36**, 1035 (2007).

11. B. H. Oh, S. Y. Jang, Prediction of diffusivity of concrete based on simple analytic equations. *cement and concrete research* **34**, 463 (2004).

12. G. Choudalakis, A. D. Gotsis, Permeability of polymer/clay nanocomposites: A review. *European Polymer Journal* **45**, 967 (2009).

13. T. Attin, F. Paque, F. Ajam, Á. M. Lennon, Review of the current status of tooth whitening with the walking bleach technique. *International endodontic journal* **36**, 313 (2003).

14. J. J. Ten Bosch, J. C. Coops, Tooth color and reflectance as related to light scattering and enamel hardness. *Journal of dental research* **74**, 374 (1995).

15. P. Sun *et al.*, Tooth whitening with hydrogen peroxide assisted by a direct-current cold atmospheric-pressure air plasma microjet. *Plasma Science, IEEE Transactions on* **38**, 1892 (2010).

16. A. Joiner, The bleaching of teeth: a review of the literature. *journal of dentistry* **34**, 412 (2006).

17. B. A. Matis, M. A. Cochran, G. Eckert, Review of the Effectiveness of Various Tooth-Whitening Systems. *Operative Dentistry* **34**, 230 (2009).

18. T. M. Auschill, E. Hellwig, S. Schmidale, A. Sculean, N. B. Arweiler, Efficacy, side-effects and patients' acceptance of different bleaching techniques (OTC, in-office, at-home). *Operative Dentistry* **30**, 156 (2005).

19. A. Joiner, Whitening toothpastes: A review of the literature. *Journal of Dentistry* **38**, e17 (2010).

20. A. Joiner, A silica toothpaste containing blue covarine: a new technological breakthrough in whitening. *International dental journal* **59**, 284 (2009).

21. D. C. Sarrett, Tooth whitening today. *The Journal of the American Dental Association* **133**, 1535 (2002).

22. British Academy of Cosmetic Dentists. (2009), BACD - Statistics. www.bacd.com.

23. iData Research (2011), U.S. Market for Dental Hygiene and Oral Care 2011. www.idataresearch.net. 2012.

24. R. H. Leonard Jr, V. B. Haywood, C. Phillips, Risk factors for developing tooth sensitivity and gingival irritation associated with nightguard vital bleaching. *Quintessence international (Berlin, Germany: 1985)* **28**, 527 (1997).

25. S. Cohen, C. Chase, Human pulpal responses to bleaching products on vital teeth. *Journal of Endodontics* **5**, 134 (1979).

26. D. Nathanson, C. Parra, Bleaching vital teeth: A review and clinical study. *Compendium (Newtown, Pa.)* **8**, 490 (1987).

27. J. R. Schulte, D. B. Morrissette, E. J. Gasior, M. V. Czajewski, The effects of bleaching application time on the dental pulp. *The Journal of the American Dental Association* **125**, 1330 (1994).

28. L. Tam, Clinical trial of three 10% carbamide peroxide bleaching products. *Journal-Canadian Dental Association* **65**, 201 (1999).

29. C. J. Tredwin, S. Naik, N. J. Lewis, C. Scully, Hydrogen peroxide tooth-whitening (bleaching) products: review of adverse effects and safety issues. *British dental journal* **200**, 371 (2006).

30. G. N. Glickman, H. Frysh, F. L. Baker, Adverse response to vital bleaching. *Journal of Endodontics* **18**, 351 (1992).

31. L. Zach, Pulp response to externally applied heat. *Oral Surg Oral Med Oral Pathol* **19**, 515 (1965).

32. S. Friedman, I. Rotstein, H. Libfeld, A. Stabholz, I. Heling, Incidence of external root resorption and esthetic results in 58 bleached pulpless teeth. *Dental Traumatology* **4**, 23 (1988).

33. A. Nanci, *Ten Cate's oral histology: development, structure, and function*. (Mosby St. Louis, Missouri, USA, 2003).

34. S. N. White *et al.*, Biological organization of hydroxyapatite crystallites into a fibrous continuum toughens and controls anisotropy in human enamel. *Journal of dental research* **80**, 321 (2001).

35. A. G. Fincham *et al.*, Evidence for amelogenin" nanospheres" as functional components of secretory-stage enamel matrix. *Journal of structural biology* **115**, 50 (1995).

36. T. M. Smith, A. J. Olejniczak, D. J. Reid, R. J. Ferrell, J. J. Hublin, Modern human molar enamel thickness and enamel–dentine junction shape. *Archives of oral biology* **51**, 974 (2006).

37. M. Staines, W. H. Robinson, J. A. A. Hood, Spherical indentation of tooth enamel. *Journal of materials science* **16**, 2551 (1981).

38. G. H. Dibdin, D. F. G. Poole, Surface area and pore size analysis for human enamel and dentine by water vapour sorption. *Archives of Oral Biology* **27**, 235 (1982).

39. J. Chu, Quantitative study of fluoride transport during subsurface dissolution of dental enamel. *Journal of Dental Research* **68**, 32 (1989).

40. D. H. Pashley, Clinical correlations of dentin structure and function. *The Journal of prosthetic dentistry* **66**, 777 (1991).

41. J. H. Kinney, M. Balooch, S. J. Marshall, G. W. Marshall, T. P. Weihs, Hardness and Young's modulus of human peritubular and intertubular dentine. *Archives of Oral Biology* **41**, 9 (1996).

42. E. Vennat, C. Bogicevic, J. M. Fleureau, M. Degrange, Demineralized dentin 3D porosity and pore size distribution using mercury porosimetry. *Dental Materials* **25**, 729 (Jun, 2009).

43. D. H. Pashley, M. J. Livingston, Effect of molecular size on permeability coefficients in human dentine. *Archives of Oral Biology* **23**, 391 (1978).

44. W. H. Bowles, Z. Ugwuneri, Pulp chamber penetration by hydrogen peroxide following vital bleaching procedures. *Journal of Endodontics* **13**, 375 (1987).

45. A. Adibfar, A. Steele, C. D. Torneck, K. C. Titley, D. Ruse, Leaching of hydrogen peroxide from bleached bovine enamel. *Journal of endodontics* **18**, 488 (1992).

46. O. Gökay, A. Müjdeci, E. Algin, In vitro peroxide penetration into the pulp chamber from newer bleaching products. *International Endodontic Journal* **38**, 516 (2005).

47. O. Gökay, F. Yilmaz, S. Akin, M. Tunçbìlek, R. Ertan, Penetration of the pulp chamber by bleaching agents in teeth restored with various restorative materials. *Journal of Endodontics* **26**, 92 (2000).

48. O. Gökay, M. Tuncbilek, R. Ertan, Penetration of the pulp chamber by carbamide peroxide bleaching agents on teeth restored with a composite resin. *Journal of oral rehabilitation* **27**, 428 (2000).

49. A. R. Benetti, M. C. Valera, M. N. G. Mancini, C. B. Miranda, I. Balducci, In vitro penetration of bleaching agents into the pulp chamber. *International Endodontic Journal* **37**, 120 (2004).

50. I. Rotstein, Y. Torek, I. Lewinstein, Effect of bleaching time and temperature on the radicular penetration of hydrogen peroxide. *Dental Traumatology* **7**, 196 (1991).

51. J. Camps, H. de Franceschi, F. Idir, C. Roland, Time-course diffusion of hydrogen peroxide through human dentin: clinical significance for young tooth internal bleaching. *Journal of Endodontics* **33**, 455 (2007).

52. L. D. Carrasco, D. M. Zanello Guerisoli, J. D. Pécora, I. C. Fröner, Evaluation of dentin permeability after light activated internal dental bleaching. *Dental Traumatology* **23**, 30 (2007).

53. C. R. G. Torres, A. Wiegand, B. Sener, T. Attin, Influence of chemical activation of a 35% hydrogen peroxide bleaching gel on its penetration and efficacy--In vitro study. *Journal of dentistry* **38**, 838 (2010).

54. W. C. Outhwaite, M. J. Livingston, D. H. Pashley, Effects of changes in surface area, thickness, temperature and post-extraction time on human dentine permeability. *Archives of Oral Biology* **21**, 599 (1976).

55. S. E. A. Camargo, M. C. Valera, C. H. R. Camargo, M. N. Gasparoto Mancini, M. M. Menezes, Penetration of 38% hydrogen peroxide into the pulp chamber in bovine

and human teeth submitted to office bleach technique. *Journal of Endodontics* **33**, 1074 (2007).

56. O. Gökay, A. Müjdeci, E. Algın, Peroxide penetration into the pulp from whitening strips. *Journal of Endodontics* **30**, 887 (2004).

57. C. T. Hanks, J. C. Fat, J. C. Wataha, J. F. Corcoran, Cytotoxicity and dentin permeability of carbamide peroxide and hydrogen peroxide vital bleaching materials, in vitro. *Journal of dental research* **72**, 931 (1993).

58. C. Hannig, H. C. Weinhold, K. Becker, T. Attin, Diffusion of peroxides through dentine in vitro with and without prior use of a desensitizing varnish. *Clinical oral investigations* **15**, 863 (2011).

59. A. Datta, V. Rakesh, An introduction to modeling of transport processes: applications to biomedical systems. *Recherche* **67**, 02 (2009).

60. S. Satish *et al.*, Modeling Peroxide Release Dynamics and Pulp Penetration during Tooth-Bleaching Procedures. (2010).

61. D. H. Pashley, V. Michelich, T. Kehl, Dentin permeability: effects of smear layer removal. *The Journal of prosthetic dentistry* **46**, 531 (1981).

62. Z. Y. Jiang, J. V. Hunt, S. P. Wolff, Ferrous ion oxidation in the presence of xylenol orange for detection of lipid hydroperoxide in low density lipoprotein. *Analytical biochemistry* **202**, 384 (1992).

63. I. Rotstein, Role of catalase in the elimination of residual hydrogen peroxide following tooth bleaching. *Journal of Endodontics* **19**, 567 (1993).

64. A. Sagiv, A. Brosh, G. Z. Ecker, Effect of Sherwood number on critical constants of diffusion. *International journal of heat and mass transfer* **41**, 1729 (1998).

65. E. W. Thiele, Relation between catalytic activity and size of particle. *Industrial & Engineering Chemistry* **31**, 916 (1939).

66. G. A. Truskey, F. Yuan, D. F. Katz, *Transport phenomena in biological systems*. (Pearson/Prentice Hall, 2004).

67. E. J. Burke, E. C. Moreno, Diffusion fluxes of tritiated water across human enamel membranes. *Archives of oral biology* **20**, 327 (1975).

68. E. R. Van der Graaf, J. J. Ten Bosch, The uptake of water by freeze-dried human dentine sections. *Archives of Oral Biology* **35**, 731 (1990).

69. E. R. Van der Graaf, J. J. Bosch, Temperature dependence of water transport into the mineralized matrix of freeze-dried human dentine. *Archives of oral biology* **36**, 177 (1991).

70. M. A. Fernández-Seara, S. L. Wehrli, F. W. Wehrli, Diffusion of exchangeable water in cortical bone studied by nuclear magnetic resonance. *Biophysical journal* **82**, 522 (2002).

71. M. Braden, R. Duckworth, S. Joyston-Bechal, The uptake of 24Na by human dental enamel. *Archives of oral biology* **16**, 367 (1971).

72. F. N. Hattab, Diffusion of fluorides in human dental enamel< i> in vitro</i>. *Archives of Oral Biology* **31**, 811 (1986).

73. M. Sulieman, M. Addy, J. S. Rees, Surface and intra-pulpal temperature rises during tooth bleaching: an in vitro study. *British dental journal* **199**, 37 (2005).

74. M. K. C. Mengel, A. E. Stiefenhofer, E. Jyväsjärvi, K. D. Kniffki, Pain sensation during cold stimulation of the teeth: differential reflection of A [delta] and C fibre activity? *Pain* **55**, 159 (1993).